Dynamics of cAMP-Dependent Protein Kinase

David A. Johnson,[†] Pearl Akamine,[‡] Elzbieta Radzio-Andzelm,[‡] Madhusudan,[‡] and Susan S. Taylor*[,‡,Δ]

Department of Chemistry and Biochemistry, Howard Hughes Medical Institute, University of California at San Diego (UCSD), 9500 Gilman Drive, La Jolla, California 92093-0654, and Division of Biomedical Sciences, University of California at Riverside, Computer Statistics Building, Riverside, California 92521-0121

Received April 12, 2001

Contents

I. Introduction

Protein phosphorylation, first elucidated as a regulatory mechanism in 1955,[1] is very likely the most important mechanism for regulation in mammalian cells. While allosteric regulation allows enzymes to respond to their immediate environment, protein phosphorylation provides a mechanism for cells to respond to external stimuli such as hormones, neurotransmitters, or any type of stress. The family of protein kinases is large and diverse.[2] On the basis of the *C. elegans* genome, protein kinases are predicted to constitute approximately 2% of the human genome,[3] and approximately a third of all proteins in mammalian cells are phosphorylated. The protein kinases serve as molecular switches and are thus by definition highly dynamic proteins that can toggle between different conformational states. Their activation state also determines who their partners are, whether their protein:protein interactions are intramolecular or intermolecular. Most protein kinases are also phosphoproteins, and those phosphates are an integral determinant for both structure and function. Phosphorylation sites can serve as docking sites for other proteins or as organizing points that lock the kinase itself into a conformation that is optimal either for catalysis or for inhibition. Correct assembly of the active kinase often depends on the critical addition of a phosphate. Thus, we have proteins that are capable of undergoing multiple conformational changes, making multiple protein:protein interactions and, in addition, nucleating the assembly of dynamic signaling complexes.

Within the large and very diverse family of protein kinases, cAMP-dependent protein kinase (cAPK), first characterized in 1968,[4] is one of the simplest and best understood.[5−7] Consequently, it often serves as a prototype for the entire family.[8,9] Its simplicity derives from the fact that it is comprised of two different types of subunits that can dissociate upon activation by cAMP.[10] Both subunit types can be overexpressed in *E. coli* as fully active proteins,[11,12] and both can be purified in large quantities. The inactive holoenzyme consists of two regulatory (R) and two catalytic subunits. The cooperative binding of cAMP with high affinity to tandem cAMP-binding domains in the R subunit induces a conformational change that unleashes the active catalytic subunits.[13] In addition to serving as inhibitors of the catalytic subunit and receptors for cAMP, the R subunits function as adapters that link the catalytic moiety via a dimerization/docking (D/D) domain to scaffold proteins termed A-kinase anchoring proteins (AKAPs).[14−16] These AKAPs target cAPK to specific subsites within the cell. The heat-stable protein kinase inhibitor (PKI) represents another class of physiological inhibitors of the catalytic subunit.[17] Like the R subunits, PKI binds with high affinity to the free catalytic subunit, but unlike the R subunit,

* To whom correspondence should be addressed. Phone: (858) 534-3677. Fax: (858) 534−8193. E-mail: staylor@ucsd.edu.
[†] University of California at Riverside.
[‡] University of California at San Diego.
[Δ] Howard Hughes Medical Institute.

10.1021/cr000226k CCC: $36.00
Published on Web 08/08/2001

David Johnson is Professor of Biomedical Sciences at the University of California, Riverside. He received his Ph.D. degree in Pharmacology from the University of California, San Francisco. He carried out postdoctoral studies in the Pharmacology and Biochemistry/Biophysics Departments at the University of California, San Francisco, and the Pharmacology Department at the University of California, San Diego. Dr. Johnson's research focuses on the development of use of fluorescence spectroscopic methods to understand how small molecules, peptides, and heteroproteins regulate the conformational and functional activity of large proteins and lipid membranes.

Elizbieta Radzio-Andzelm joined the Department of Chemistry and Biochemistry at the University of California, San Diego, in 1992 as a postdoctoral research fellow. She completed both her M.S. and Ph.D. degrees with honors in Chemistry from the University of Warsaw, Poland. Her interests in molecular interactions took her to the University of Alberta, Canada, and later to the University of Montreal, where she performed quantum chemical calculations for molecules using GAUSSIAN and other programs. Currently a UCSD Staff Research Associate, Dr. Radzio-Andzelm continues to study protein structure using homology models, molecular mechanics, and dynamic simulations.

Pearl Akamine is a graduate student at the University of California, San Diego, in the Department of Chemistry and Biochemistry. She received her B.S. degree from the University of California, San Diego, in Physics-Biophysics. She is currently using X-ray crystallography to study the requirements for ligand binding of the catalytic subunit of the cAMP-dependent protein kinase.

Dr. Madhusudan received his M.S. degree in Physics from the University of Delhi and his Ph.D. degree in Structural Biology from the Indian Institute of Science at Bangalore, India. He relocated shortly thereafter to the United States and joined the Department of Molecular and Experimental Medicine at The Scripps Research Institute of La Jolla, CA. Dr. Madhusudan divided his years as a postdoctoral fellow between Scripps and the Howard Hughes Medical Institute, where he worked in the Department of Chemistry and Biochemistry. His strengths in structural biology, bioinformatics, and software development have lead to a recent new appointment with the San Diego Supercomputer Center, located on the campus of the University of California, San Diego.

it includes a nuclear export signal (NES) that mediates active nuclear export of the catalytic subunit.[18]

In considering the dynamics of cAPK, it is essential to use a variety of methods and to consider multiple levels of dynamics. Specifically, we will consider the molecules that are associated with catalysis, inhibition, and targeting. The physical properties of these three classes of proteins differ substantially. Initially we will focus on the dynamics of the globular catalytic subunit. The discussion will include the conserved core and the motions that are associated with the catalytic cycle as well as the dynamics of the non-conserved tails that flank the core at the C- and N-termini. Next will be a review of the inhibitors of the catalytic subunit—specifically, the heat-stable protein kinase inhibitor and the regulatory subunits. These multidomain proteins are multifunctional and show significant regions of disorder. We will focus in particular on the dynamics and multifunctionality of the R subunits and on the dynamic structure and function of PKI. Finally, it is not sufficient to simply have an active kinase, that kinase must be in the correct part of the cell at the correct time to mediate its correct biological responses. Thus, the anchoring of cAPK by modular scaffold proteins, AKAPs, also will be discussed. This adds a new dimension to the integration of cellular signaling by cAPK and emphasizes that in considering the function of a protein kinase within a living cell, space as well as time contributes to dynamics.

Our goals are not simply to describe the highly dynamic features of each of these proteins, but also to focus on the diversity of methods, summarized in Table 1, that have been used to characterize and understand their dynamic properties. X-ray crystallography is essential for defining high-resolution

Susan Taylor is Professor of Chemistry and Biochemistry at the University of California, San Diego, a Howard Hughes Medical Institute Investigator, and a Senior Fellow of the San Diego Supercomputer Center. She received her B.A. degree in Chemistry from the University of Wisconsin and her Ph.D. degree in Physiological Chemistry from the Johns Hopkins University. She carried out postdoctoral studies at the Medical Research Council Laboratory of Molecular Biology in Cambridge, England, and at the University of California, San Diego. She served as President of the American Society of Biochemistry and Molecular Biology. She is a member of the American Academy of Arts and Sciences, the National Institute of Medicine, and the National Academy of Sciences. Dr. Taylor's research is focused on the structure and function of protein kinases with cAMP-dependent protein kinase serving as a prototype for the entire family of over 2000 protein kinases. She has used interdisciplinary approaches that extend from obtaining high-resolution structures of the proteins to using fluorescence strategies to follow the dynamic movements of the enzyme in cells.

structures—especially for the larger proteins. The catalytic subunit has been well characterized crystallographically. Where sufficient resolution exists, some insight into the structural order and/or flexibility can be gained from the crystal structures. New NMR methods are capable, in principle, of solving large structures (TROSY).[19] Although NMR has been used to solve the structures of small domains and motifs in the regulatory subunits and PKI, the structures of full-length subunits of cAPK have not yet been solved by NMR. Eventually we hope to see NMR structures of some of these more asymmetric molecular assemblies where one could better appreciate at high resolution the conformational flexibility of these proteins. In the interim, X-ray crystallography provides only snapshots of specific conformations; however, it is usually not possible to form crystals of all functional conformations and configurations of the proteins under study. Furthermore, the crystal structures provide little insight into the equilibrium between different conformational states in solution. The crystal structures thus need to be complemented by other solution methods. NMR, fluorescence spectroscopy, hydrogen/deuterium exchange coupled with mass spectroscopy, and small-angle X-ray scattering are complimentary methods that have been used to characterize cAPK in solution. As indicated in Table 1, these methods either cover a specific time frame(s) or detect state-dependent shifts in equilibrium structural features. These windows of time or equilibrium structural features differ for catalysis, inhibition, and targeting.

II. Catalytic Subunit

The catalytic subunit of cAPK is comprised of a bilobal core that is shared by all members of the protein kinase superfamily.[20] The ribbon representation in Figure 1 is color-coded according to the conserved sequence motifs first identified by Barker and Dayhoff[21] and subsequently analyzed in great detail for the protein kinase superfamily by Hanks and Hunter.[2,22] The color-coded sequences corresponding to regions I−XI, as defined by Hanks, are also indicated as are the highly conserved residues that are distributed throughout the core. These conserved residues are essentially superimposable in all members of the protein kinase superfamily when the enzymes are in their active conformation.[23−25] Mostly the conserved residues cluster around the active site cleft and contribute to nucleotide binding and/or phosphoryl transfer. However, these residues are also part of a network that extends throughout the entire molecule.[8]

In the catalytic subunit, the conserved core is flanked by a 40-residue acylated and mostly helical

Table 1. Solution Methods for Measuring Dynamics

solution methods	time scale	comments
NMR	ps−ns; μs−ms	**Heteronuclear (^{2}H, ^{13}C, and ^{15}N) spin relaxation** measurements permit the characterization of backbone and side chain dynamic properties of proteins. Less quantitative dynamic information comes out of comparison of multidimensional NMR **structures** associated with equilibrium solution conditions.
fluorescence	ps−ns; μs−h	**Time-resolved anisotropy** monitors the time course of reorientation following photoselective excitation of reporter groups (endogenous or conjugates) to yield information on local, segmental, and global diffusion in the ps to ns time domain. **Förester resonance energy transfer** techniques typically yield discrete intersite distances or distances of closest approach in the μs to min time domain. Distribution of distances can be measured in the ps to ns time domain.
CD spectroscopy	ms−h	**Circular dichroism** monitors differential absorption of left- and right-hand circularly polarized light to yield information on the secondary structure of macromolecules. Dynamic information is typically deduced from differences in structure associated with equilibrium solution conditions.
small-angle scattering	ms−h	**Small-angle (X-ray or neutron) scattering** data yields time-averaged low-resolution structural information. Dynamic information comes out of changes in structure associated with equilibrium solution conditions or from time-resolved measurements made using synchrotron radiation.
H/D exchange by mass spectrometry	ms−h	**Amide hydrogen exchange** uses a quench/protease fragmentation methodology and subsequent analysis by mass spectrometry to assess structural dynamics of solvent exposed surfaces.

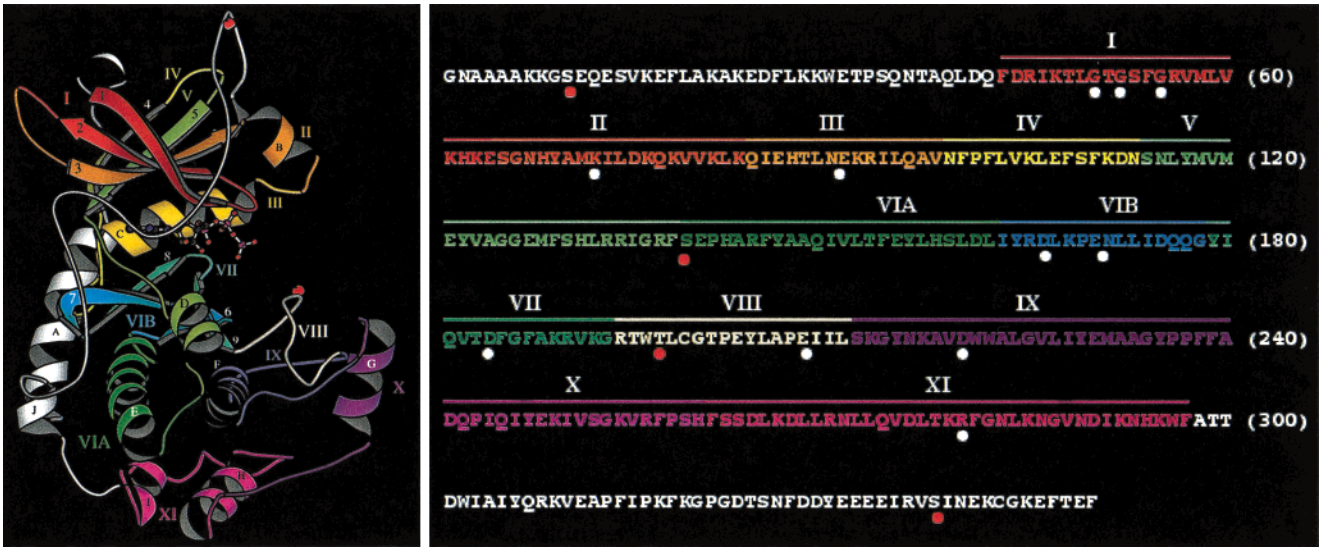

Figure 1. Fold and sequence motifs of a catalytic subunit of cAPK. The ribbon diagram of the catalytic subunit (left) is taken from the coordinates of the ternary complex containing ATP and PKI(5−24) (1ATP). Phosphorylation sites at Ser338 and Thr197 are indicated as red dots. The coloring of the conserved core (residues 40−300) correlates with the Hanks and Hunter designation of conserved regions (I−XI) of the protein kinase family.[2] The color-coded sequence is on the right. Conserved residues are indicated by white dots.

Table 2. Crystal Structures of C-Subunit Complexes

PDB code (conformation)	complex/resolution (Å)	ligand(s)	species (m/r)[b]	ref
1CMK	binary	iodinated PKI(5−24)	Porcine (m)	57
open	2.9			
1ATP	ternary	Mn_2ATP	Murine (r)	26
closed	2.2	PKI(5−24)		
1CDK	ternary	Mn_2AMPPNP	Porcine (m)	173
closed	2.0	PKI(5−24)		
1APM	binary	PKI(5−24)	Murine (r)	174
closed	2.0			
1CTP	binary	di-iodinated PKI(5−24)	Porcine (m)	53
open	2.9			
1STC	ternary	staurosporine	Bovine (r)	175
intermediate	2.3	PKI(5−24)		
1YDR	ternary	H7[c]	Bovine (r)	176
closed	2.2	PKI(5−24)		
1YDS	ternary	H8[d]	Bovine (r)	176
closed	2.2	PKI(5−24)		
1YDT	ternary	H89[e]	Bovine (r)	176
closed	2.3	PKI(5−24)		
1FMO	ternary	adenosine	Murine (r)	43
closed	2.6	PKI(5−24)		
1BKX	binary	adenosine	Murine (r)	54
intermediate	2.6			
1BX6	binary	balanol	Murine (r)	177
intermediate	2.2			
1JBP	ternary	ADP	Murine (r)	178
closed	2.2	PKS(5−24)		
ND[a]	binary	phosphoryl PKS(5−24)	Murine (r)	178
closed	2.3			

[a] Refers to coordinate sets not deposited in protein data bank. [b] m represents mammalian expression and r recombinant expression. [c] 1-(3 Isoquinolinesulfonyl)-2-methylpiperazine. [d] [*N*-(2-Methylamino)ethyl]-5-isoquonolinesulfonamide. [e] *N*-[2-(*p*-Bromocinnamylamino)ethyl]-5-isoquinolinesulfonamide.

motif at the N-terminus and by a 50-residue extended tail at the C-terminus that spans the surface of both core domains and is highly disordered near the end in the absence of ligands.[20] The nucleotide lies at the base of the cleft between the two lobes,[26] while the peptide docks onto a ledge that is provided by the large lobe.[27]

Our review will focus first on the conserved core and then on the flanking segments. Our structural comparisons are based upon 14 crystal structures which represent both mammalian (m) and recombinant (r) enzymes in various liganded states (Table 2). The catalytic subunit has been crystallized in complex with a variety of peptides, nucleotides, and inhibitors. These structures not only define the substrate and inhibitor binding sites, but also provide clues about the conformational malleability of the protein and the nature of ligand-induced conformational changes.

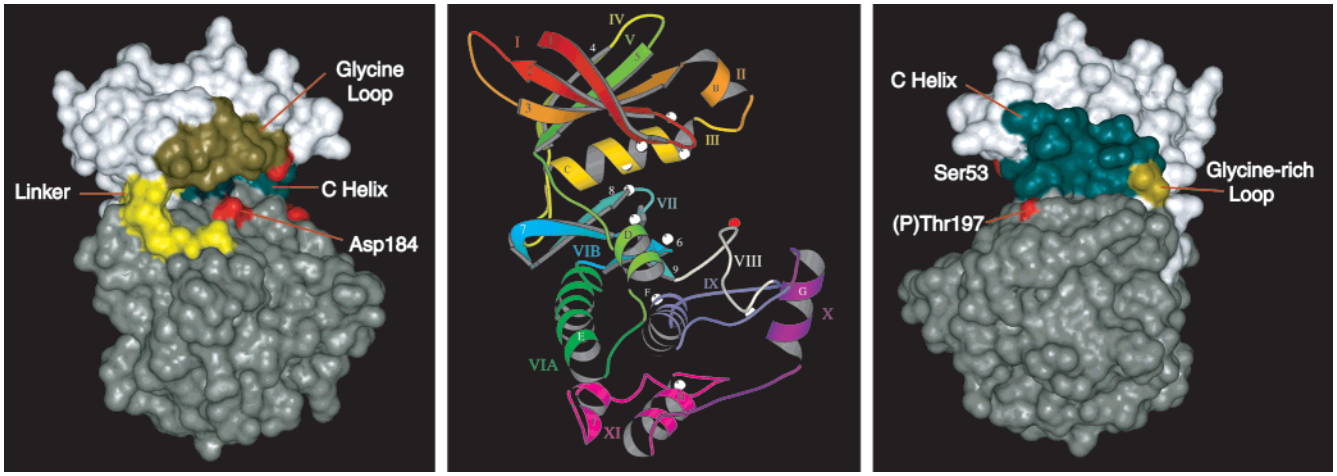

Figure 2. Conserved core of the catalytic subunit. The conserved core of the mammalian enzyme:PKI(5−24) complex (1CMK), residues 40−300, shows an open conformation. The small lobe (residues 40−119) is white; the linker (residues 120−127) is yellow; the large lobe (residues 128−300) is gray. The glycine-rich loop (residues 46−57) is gold with Ser53 at the tip of the loop highlighted in red. Phospho-Thr197 at the edge of the active site cleft and Asp184 on the floor of the active site cleft are also highlighted in red. The C helix is shown in dark green. The view on the left reveals the open cleft where ATP docks, while the view on the right, rotated by 180°, reveals the exposed back surface of the C helix when the C-terminal and N-terminal tails are stripped away. In the middle panel is a ribbon diagram of the core only, showing the conserved Hanks motifs. The white balls are the residues that are conserved throughout the protein kinase family.

A. Core Domains

The conserved core, shared by all Ser/Thr- and Tyr-specific protein kinases, illustrated in Figure 2, is comprised of two domains that have different functional roles and dynamic characteristics.[9] When expressed in *E. coli*, the catalytic subunit is autophosphorylated,[28] and thus, the recombinant enzymes that have been studied in depth so far have always been in an active state. Unlike most other protein kinases, no structure of an inactive, dephosphorylated enzyme has been solved; the conformation of the inactive, nonphosphorylated enzyme is unknown. As summarized in Table 2, X-ray structures of the catalytic subunit with various ligands have been solved, but in all cases Thr197 in the activation loop and Ser338 near the C-terminus are phosphorylated. The conformational changes that we observe in the catalytic subunit are thus assumed to reflect normal fluctuations that the enzyme is capable of undergoing in the process of catalysis.

Overall, the small lobe provides the major docking site for ATP while the large lobe has an exposed docking surface for the peptide/protein substrate. The base of the cleft between the two lobes forms a deep, mostly hydrophobic, pocket for the adenine ring of ATP. The wedge-shaped cleft, lined by the glycine-rich loop and the C helix in the small lobe and by the β sheet in the large lobe, positions the γ-phosphate for transfer while the residues that position the peptide to accept the phosphate are part of the large lobe. Asp184 in the large lobe plays a unique role at the interdomain surface by positioning the magnesium ion that bridges the β- and γ-phosphates of ATP. This positioning draws the γ-phosphate toward the peptide acceptor. Most of the highly conserved residues that characterize this enzyme family are clustered around the active site cleft and contribute either to the binding of ATP or to facilitating the transfer of the γ-phosphate. In general, the small lobe is more malleable whereas the large lobe appears to be quite stable and undergoes no major ligand-induced conformational changes once the enzyme is phosphorylated.

1. Small Lobe

The small lobe is comprised of a conserved five-stranded antiparallel β sheet with a conserved helix spanning the domain between β-strands 3 and 4 (Figure 3, top left). In cAPK, these conserved elements constitute β-strands 1−5 and the C helix. The specific conserved motifs in the small lobe include the glycine-rich loop, β-strand 3, and the C helix (Table 3). With the exception of the loop between the C helix and β-strand 4 that is anchored firmly to the large lobe, the small lobe is largely uncoupled from the large lobe. The only direct ionic interaction is between His87 at the beginning of the C helix and phospho-Thr197 in the activation loop of the large lobe, and this occurs in the closed conformation. The interactions between the small and large lobes are largely mediated by ATP, which acts like a glue that harnesses the lobes together. In the absence of ATP, the two lobes are relatively uncoupled. One can appreciate this most fully when only the core is considered. Without the N- and C-termini and in the absence of ATP, there is very little to hold the two lobes together.

Two different representative structures, shown in Figure 4, compare "closed" and "open" conformations. When only the small lobes (residues 40−120) from the different structures are superimposed, there are remarkably few differences. The exception is the glycine-rich loop between β-strands 1 and 2. This hallmark feature of the family was identified almost immediately as part of the ATP-binding site; however, the subsequent elucidation of additional structures as well as kinetic and mutagenesis studies have revealed that this loop is an essential part of the catalytic machinery.[29−32] Although this loop embraces the entire nucleotide, its primary function is to

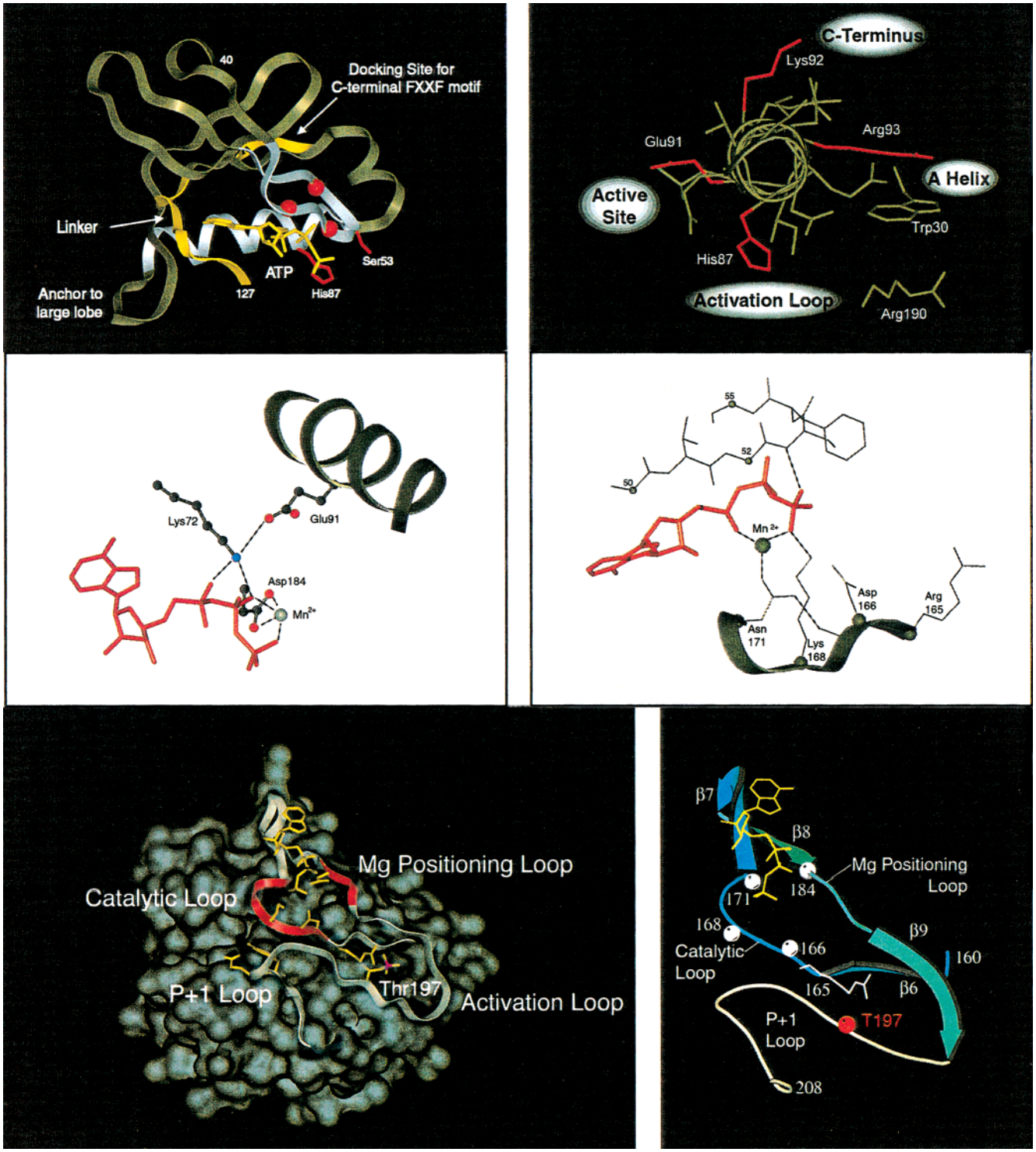

Figure 3. Structural motifs in the small and large lobes of the conserved core of the catalytic subunit of cAPK. The conserved motifs in the small lobe (top) and large lobe (bottom) are highlighted. In the small lobe (top left) the two dominant motifs, the glycine-rich loop and the C helix, are shown in white, while the conserved glycines in the loop, 50, 52, and 55, are shown as red balls. The linker (residues 120−127) is shown in yellow, as are the four C-terminal residues (residues 347−350) that are anchored to the small lobe by Lys92 in the C helix. The position of the ATP in the ternary complex (1ATP) is also shown. The view on the left emphasizes that the C helix spans the breadth of the small domain at the cleft interface from the linker to His87 which hydrogen bonds to phospho-Thr197 in the large lobe when the cleft is closed. On the right top is an end-on view of the C helix highlighting the many contacts that residues in this helix make with other parts of the protein. A surface view of the large lobe at the bottom left shows the β sheet that lines the wall of the active site cleft (residues 160−208). The definition of the strands and motifs and loops is indicated on the bottom right. In the center, the key interactions that take place during catalysis at the active site cleft are highlighted. On the middle left is the positioning of the γ-phosphate of ATP by the concerted actions of Lys72 and Glu91 in the small lobe and Asp184 in the large lobe. On the middle right is the presumed transition state in phosphoryl transfer where the γ-phosphate is anchored by the backbone amide of Ser53 in the glycine-rich loop in the small lobe and the side chain of Lys168 in the catalytic loop of the large lobe.

Table 3. Protein Kinase Motifs: Small Lobe

motif/amino acid	2° structure	subdomain	function
glycine-rich loop	***β*1-loop-*β*2**	**I**	
Lys47			anchors C-terminal tail
Thr48			anchors C-terminal tail
			anchors Arg56 in *β*−strand 2
Gly50			helps to anchor α−phosphate
Gly52			positions amide of Ser53
Ser53			goes to *γ*-phosphate
			goes to P Site carbonyl in peptide
Phe54			helps to exclude water from the site of phosphoryl transfer
Gly55			anchors *β*-phosphate
Arg56			anchors to *β*-strand 3
			anchors to Thr48 in *β*-strand 1
			anchors C-terminal tail
Val57			hydrophobic cap for adenosine
Lys72	***β*3**	**II**	anchors α- and *β*-phosphates of ATP
			bridge to Glu91 in C helix
C helix	**C helix**	**III**	
Gln84			anchors His87
His87			bridge to Thr197 in activation loop
Glu91			bridge to Lys72 and active site
Lys92			anchoring of C-terminus carboxyl
			anchors Glu34
Arg93			anchor to A helix and N-terminus
Gln96			anchoring the N-terminus to small lobe through Ser34 and Lys29
Phe100-Phe102	**αC−*β*4 Loop**	**IV**	hydrophobic anchor to large lobe
			anchor for acyl-binding pocket

Amino acids in bold are conserved throughout the protein kinase superfamily.

position the *γ*-phosphate of ATP for phosphoryl transfer. The essential contact is between the backbone amide of Ser53 at the tip of the loop and the *γ*-phosphate. In the various crystal structures of the catalytic subunit, this loop is only stable with low-temperature factors in the fully closed conformation, which is found in the PKI (5−24):ATP [26] and PKI (5−24):AMPPNP ternary complexes.[29] Of the three glycines (50, 52, and 55), Gly52 is the most essential based on Ala scanning mutagenesis of the loop and on modeling of steric constraints that would be introduced by an additional methyl group.[31,33] In this fully closed conformation, the *γ*-phosphate of ATP is within hydrogen-bonding distance of the backbone amide of Ser53 at the tip of the glycine-rich loop (Figure 3, middle right). Although the side chain of Ser53 also hydrogen bonds to the backbone amide and backbone carbonyl of the P-site residue in the peptidyl substrate, this side chain interaction is not essential for catalysis; replacement of Ser53 with Gly has no major effect upon catalysis.[32]

In addition to the glycine-rich loop, there are two conserved charged residues in this lobe: Lys72 in *β*-strand 3 and Glu91 in the C helix. In our structures, which all reflect active enzymes, these residues face each other and are usually within hydrogen-bonding distance. Typically when a kinase such as *src*,[34,35] hck,[36,37] the insulin receptor,[38,39] or cdk2[40−42] is in an inactive conformation, the C helix is twisted so that the equivalent Glu91 side chain faces the solvent at the cleft interface.[23] In many cases, this glutamate interacts with a highly conserved Arg (Arg165 in cAPK) that precedes the catalytic loop between *β*-strands 6 and 7. When the activation loop is phosphorylated, this arginine interacts with that essential phosphate; the phosphate in the activation loop successfully out-competes for this Arg. Phosphorylation of the activation loop may thus accomplish several things. It orients the peptide-binding site, it positions the residues at the active site for optimum catalysis, and it allows the small lobe to snap into its active conformation. In the catalytic subunit, it is His87, one turn earlier in the C helix, that interacts with the phosphate on Thr197. Glu91 in all cases is facing Lys72 with distances in the various structures ranging from 2.6 to 4.1 Å.

2. Large Lobe

In contrast to the small lobe, the large lobe (residues 128−300) appears to be quite stable. In cAPK, where all of the structures so far are of the active phosphorylated enzyme, there are no obvious ligand-dependent conformational changes in the large lobe. The temperature factors for all of the α carbons in active site loops in the large lobe are consistently low; there are no major conformational changes in any of the crystal structures.[43] The large lobe contributes to the ATP-binding surface through a *β* sheet motif that is linked to the activation loop and the P+1 peptide-binding loop. This extended surface, represented in Figure 3 **(**bottom**)**, begins with *β*-strand 6 (residues 160−165) and ends with the APE (Ala-Pro-Glu) motif (residues 206−208) that anchors Glu208 to a conserved and relatively buried Arg280 near the end of the domain. The conserved loops that link and flank these *β*-strands are highly conserved and mostly contribute to the organization of the active site (Table 4). The complexity of these loops as signaling motifs is striking. Almost every residue has a specific function. In addition, these residues radiate to different parts of the protein and thus are extremely well positioned to contribute to the broader signaling network.

Catalytic Loop. The catalytic loop (Asp-Leu-Lys-Pro-Glu-Asn; residues 166−171) joining *β*-strands 6 and 7 contains several highly conserved residues with

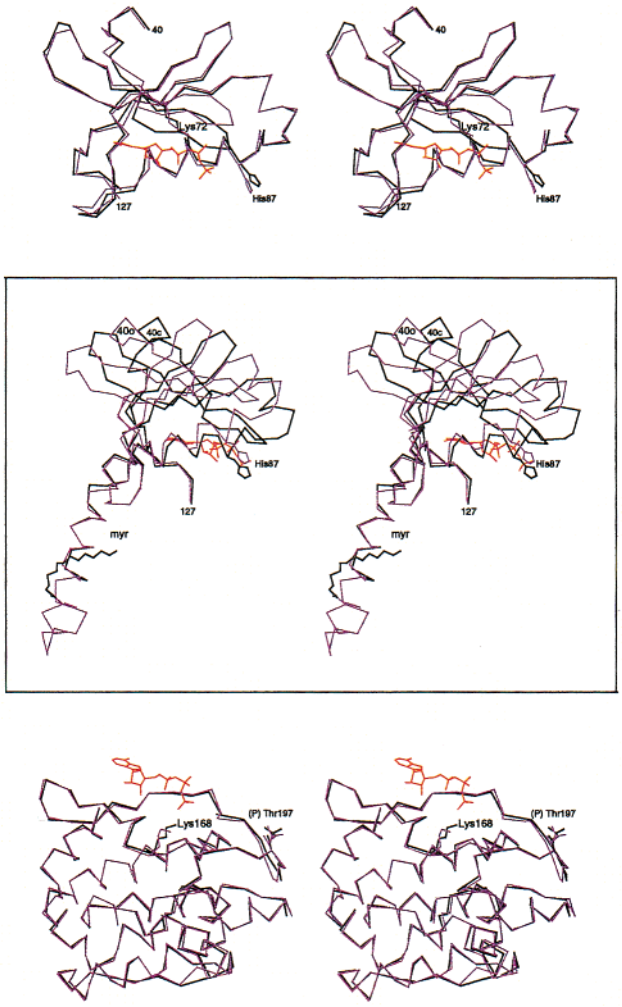

Figure 4. Domain movements in the catalytic subunit. In the top panel the small domain only is superimposed from the open binary complex (purple) of the mammalian catalytic subunit and PKI(5−24) (1CMK) and the closed ternary complex (black) of C:PKI(5−24):ATP (1ATP). ATP is red; the myristyl group, seen only in the mammalian enzyme, is black. The side chain of His87 and Lys 72 are also shown. In the bottom panel the large lobes have been superimposed. The middle panel shows the first 127 residues when the large lobes (not shown) are superimposed. The two segments that appear to be firmly anchored to the large lobe are the A helix and the αC:β4 loop (residues 96−105). In this view the motions that are associated with opening and closing of the cleft are seen. This figure has been adapted from Zheng et al.[57]

Asp166 positioned to serve as a catalytic base and Lys168 interacting with the γ-phosphate of ATP (Figure 3, middle right). Despite its proximity to the hydroxyl group of the P-site residue, Asp166 does not appear to provide major rate enhancement.[44,45] Glu170 points away from the active site cleft and is part of the binding pocket for the P-2 Arg in the peptide substrate/inhibitor. Asn171 is strictly conserved throughout the protein kinase family. It binds to the magnesium ion that bridges the α- and γ-phosphates of ATP and also interacts with the major activating magnesium ion that bridges the β- and γ-phosphates. Asn171 also hydrogen bonds through its side chain amide to the α-carbonyl of Asp166, thereby stabilizing the loop.

Magnesium Positioning Loop. The magnesium positioning loop (Asp-Phe-Gly-Phe; residues 184−187) between β-strands 8 and 9 also contributes to catalysis by Asp184 binding to the magnesium ion that bridges the β- and γ-phosphates of ATP (Figure 3, middle left). Asp184 is strategically positioned on the floor of the active site cleft where it can shuttle between the small and large lobes. As discussed later, molecular dynamics calculations indicate that this Asp tracks with the small lobe rather than the large lobe when correlated motions and rigid body movements are compared.[46] The highly conserved Phe187 helps to exclude water from the site of phosphoryl transfer. Lys72 and Glu91 in the small lobe and Asp184 in the large lobe serve as a catalytic triad at the back of the active site cleft (Figure 3, middle left). The function of this triad is to bind the phosphates of ATP and orient the γ-phosphate for transfer to a protein substrate. Lys72 and Glu91, together with the glycine-rich loop, position the phosphates, while Asp184 orients the γ-phosphate toward the substrate. Lys168 in the catalytic loop grabs the γ-phosphate from the other side. The cleft between the small and large lobe is bridged by ATP. The adenine ring fills the hydrophobic pocket, and the phosphates form a network of ionic and hydrogen-bonding interactions between the lobes. ATP thus holds the two lobes together; without ATP, there are few interactions between the two lobes.

Activation Loop. β-Strand 9 links the magnesium positioning loop to the activation loop, which is critically coordinated by the highly conserved phosphate on Thr197. In cAPK, Thr197 is phosphorylated autocatalytically during expression in *E. coli*,[28] and this phosphate, as discussed above, is always present in the structures that have been solved to date. The network of interactions that connect this phosphate to the catalytic loop and the magnesium positioning loop are shown in Figure 5 (center). The interaction of this loop with the small lobe is mediated by His87 at the beginning of the C helix, but His87 only interacts with Thr197 when the catalytic subunit is in the closed or intermediate conformation. Its link to the N-terminal A helix is through β-strand 9, where Lys189 binds to the phospho-Thr197 and Arg190 forms the pocket where Trp30 at the end of the A helix docks.

In other protein kinases, this loop is often highly disordered or in a different conformation [34−37,39−42,47] (Figure 5, bottom right). This region is frequently only ordered into an active conformation as a consequence of phosphorylation. In these cases, the rest of the large lobe is folded correctly. It is the phosphorylation of the activation loop by a heterologous protein kinase that is essential for activation.[48] For the catalytic subunit of cAPK, we have only seen the phosphorylated conformation. Phosphorylation of the catalytic subunit is mediated by a heterologous kinase,[49] possibly, PDK1,[50] a protein kinase that plays a major role in activating many AGC subfamily members.[51] Unfortunately, however, we know nothing about the conformation of the activation segment in its unmodified state.

Table 4. Protein Kinase Motifs: Large Lobe

motif/amino acid	2° structure	subdomain	function
catalytic loop	**β6−β7 loop**	**VIB**	
Arg165			bridge to the activation loop
			bridge to Mg positioning loop
			bridge to F helix via Asp220
Asp166			"catalytic base"
Lys168			bridge to γ-phosphate of ATP
Leu169			hydrophobic anchor to large lobe
Glu170			recognition site for P-2 Arg
Asn171			coordination of 2° magnesium ion
magnesium positioning loop	**β8−β9 loop**	**VII**	
Asp184			coordination of 1° magnesium ion
Phe185			shielding active site from solvent
Phe187			bridge to Arg165
	β9		
Lys189			anchor to Thr197 phosphate
Arg190			bridge between active site and A helix
activation loop	**β9-P+1 loop**	**VIII**	
Thr195			anchors Thr197; stabilize turn
Trp196			R binding surface
Thr197			assembly of active site via Arg165
			anchors to β−strand 9 via Lys189
			closing active site cleft (His87)
			anchor A helix through Lys189
peptide positioning loop	**198−205**	**VIII**	
Leu198			P+1 hydrophobic site
Gly200			docking surface for P Site backbone
			stabilizes turn through carbonyl
Thr201			contributes indirectly to phosphoryl transfer
			shuttles between Asp166 and Lys168
Pro202			P+1 hydrophobic site
Glu203			binding site for P-6 Arg
Tyr204			binding site for P-2 Arg
Leu205			P+1 hydrophobic binding site
Glu208			anchors activation segment
	F helix	**IX**	
Asp220			bridge to active site
			anchors backbone of Arg165 and Tyr164
Trp221			hydrophobic anchor to core
Trp222			anchoring of Glu208 and Arg280
Glu230			binding site for P-2 Arg
Tyr235			hydrophobic P-11 binding site
Arg280		**XI**	anchors cap of large lobe to activation segment

Peptide Positioning Loop. The segment joining the activation loop to the APE anchoring motif was referred to previously as the P+1 loop because it provides the pocket where the P+1 substrate residue docks. In cAPK, the P+1 residue is hydrophobic.[52] The binding pocket is provided by the side chains of Leu198, Pro202, and Leu205. In actuality, this loop should be more appropriately considered as the peptide positioning loop as it touches and contributes to the positioning of most parts of the consensus site substrate peptide (P-3 through P+1). Gly200 rests directly under the P-site residue in the peptide, while Thr201, conserved in Ser/Thr-specific protein kinases, hydrogen bonds by its side chain hydroxyl to the putative catalytic base, Asp166, and/or Lys168, also in the catalytic loop. Glu203 provides a docking site for the P-6 Arg, while Tyr204 contributes to organization of the site that binds the P-2 Arg. Consequently, this loop either directly or indirectly contacts at least 5 subsites of the peptide.

Glu220 and Arg280 are two additional conserved charged residues in the large lobe that contribute to the structure more indirectly, and their role has not been well studied. The domain is characterized by a very hydrophobic core that is dominated by α-helices. Two of the longest helices, the E helix and the F helix, are very hydrophobic and are unusual in that they run right through the middle of the core. Asp220, another conserved residue, lies at the beginning of the F helix and hydrogen bonds to the backbone amides of Tyr164 and Arg165. Arg280 is part of the subdomain that appears to cap the bottom of the large lobe. It forms an ion pair with Glu208 and thus appears to help stabilize the peptide-binding loop.

3. Opening and Closing of the Active Site Cleft

The opening and closing of the active site cleft serves to position the ATP for catalysis. The crystal structures reveal a variety of conformations that overall represent different stages of opening the cleft between the two lobes (Figure 4). The most open conformation is of the mammalian myristylated protein that is complexed to an iodinated form of PKI-(5−24) (PDB code 1CMK or 1CTP).[26,53] We do not know if this is the most open conformation that the catalytic subunit can assume in solution; it is simply the most open conformation that has been observed by X-ray crystallography. Consequently, for this discussion, we use this structure to represent the most open conformation. The fully closed conformation is the ternary complex of C:PKI(5−24) and ATP (PDB code 1ATP).[26] As indicated in Table 5, three

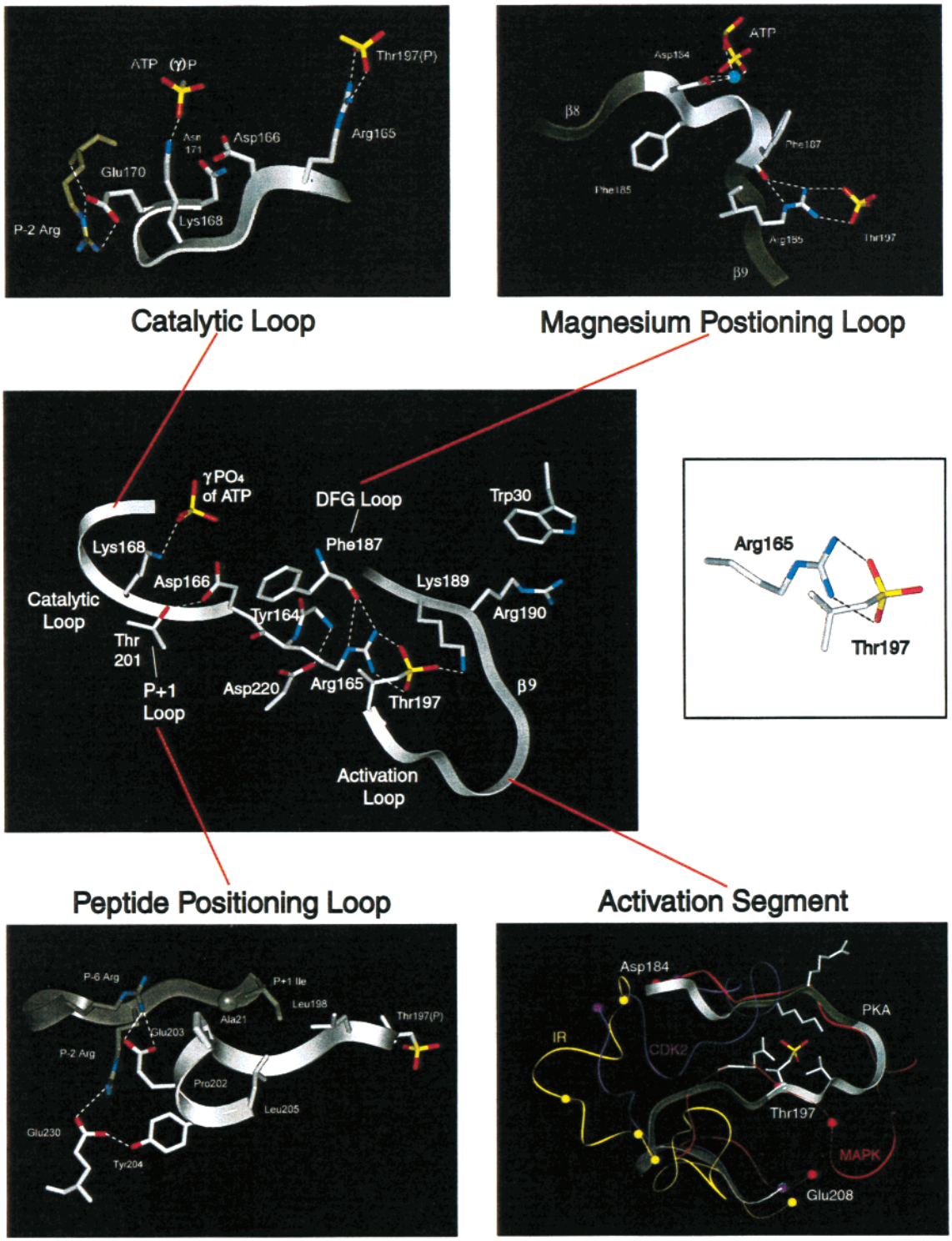

Figure 5. Integrated loops of the catalytic subunit. The center figure shows the stabilization of Arg165 at the junction of four loops—the catalytic loop, the magnesium positioning loop, the activation loop, and the peptide positioning loop. Asp220, another conserved residue that lies more distal to the active site, actually binds to the backbone amides of Tyr164 and Arg165, thus providing stabilization from one direction. The other direction is stabilized by the backbone carbonyl of Phe187 that terminates the DFG loop. Arg165 thus makes at least three major contacts with conserved residues in addition to its key role in liganding the phosphate on Thr197. The top two figures and the bottom left figure were adapted from Smith et al.[9] The bottom right figure shows the conformations that the activation loop adopts in the insulin receptor (IR) and in cdk2 when the loop is not phosphorylated.

specific distances can be used as indicators of closed and open conformations.[54−56] Glu170−Tyr330 measures the distance of the C-terminal tail to the active site. It is nearly 15 Å in the open conformation. Additionally, the tail is very disordered. The His87 to phospo-Thr197 distance measures the position of the C helix relative to the large lobe. In the closed conformation, the C helix is hydrogen bonded to the

Table 5. Parameters Indicative of Global Conformation[a]

conformation	open	intermediate	closed	closed	closed
species	porcine	mouse	mouse	mouse	porcine
peptide	PKI (5−24)*	PKI (5−24)	PKI (5−24)	PKI (5−24)	PKI (5−24)
nucleotide	none	adenosine	ATP	none	AMP−PNP
PDB code	1CTP	1BKX	1ATP	1APM	1CDK
radius of gyration (Rg)	21.0	20.3	20.0	N/A	N/A
distance between His87 and Thr197	7.1	3.2	2.7	2.8	2.8
distance between Ser53 and Gly186	14.2	11.8	10.4	10.0	10.5
distance between Glu170 and Tyr330	14.6	8.6	8.2	8.2	7.9

[a] Tyr 7 is di-iodinated. Rg was calculated using all non-hydrogen atoms of C. Inclusion of substrate peptide or peptide inhibitor increased the value of Rg by ≤0.1 Å. The atoms used for distance measurements were Nϵ2 of His87 to closest phosphate oxygen of Thr197; Cα of Ser53 to Cα of Gly186; O of Glu170 to OH of Tyr330.[54] All measurements are in Å.

phosphate of Thr197 in the activation loop. Ser53−Gly186 measures the opening and closing of the glycine-rich loop. This distance reflects H-bonding of the Ser53 amide to the γ-phosphate of ATP. An analysis of the various structures shown in Table 2 reveals that there are intermediate conformations such as adenosine:C where the C-terminal tail is snapped into its closed configuration and the C helix is also in the closed conformation; however, the glycine-rich loop is still disordered and more open.

Interestingly, binary complexes of PKI(5−24) catalytic subunits in the closed conformation have also been observed. In solution, PKI(5−24) or ATP alone may shift the equilibrium to a more closed conformation. The existence of both closed and open binary crystals of the catalytic subunit and PKI(5−24) suggest that these complexes fluctuate between open and closed states. The crystallographic evidence sheds no definitive light on the equilibrium between these states in solution.

As mentioned earlier, when the small lobes are superimposed, the unique mobility of the glycine-rich loop can be appreciated. In contrast to the temperature factors of the loops in the large lobe which are low and do not change, the temperature factors for the glycine-rich loop vary widely in the different structures.[43] Only in the ternary complex with ATP and PKI(5−24) are the temperature factors consistently low. The highest temperature factors are at the very tip of the loop corresponding to Gly52 and Ser53. Mutagenesis confirms the mechanistic importance of this segment for phosphoryl transfer.[30−32] When the open and closed conformations of both the large lobe and the small lobe are superimposed (Figure 4, middle panel), one can also appreciate that the global motion of the small lobe relative to the large lobe involves more than just the simple motions of the glycine-rich loop. Opening of the cleft is not a simple hinge movement but instead represents both a hinging and sliding motion.[43,46] While it is essential that there be at least a partial opening of the cleft to allow the ADP to be released and the ATP to bind, it has not been established whether the movement of the glycine-rich loop alone might be adequate to release the nucleotide. The open conformation seen in the mammalian binary complex most likely is not populated to any appreciable extent given the relatively high concentrations (2−10mM) of ATP and ADP within the cell, levels that are well above K_d (18 μM).[44]

B. N-Terminus/C-Terminus

The conserved core of the catalytic subunit is flanked by nonconserved segments at each end, 40 residues at the N-terminus and 50 residues at the C-terminus. The stable large lobe serves as an anchoring module for these "tails". It not only provides a docking surface for the peptide/protein substrate and for the loop between the C helix and β-strand 4 in the small domain, but also provides a hydrophobic platform that anchors the tails and brings both tails together. The C-terminal tail has a mobile component as well as a piece that is firmly anchored to the large domain and another smaller piece that is anchored to the small lobe. The N-terminus is anchored, primarily by hydrophobic contacts, to the surface of both lobes. The anchoring of the N-terminus also may be regulated by post-translational modifications and by isoform-specific holoenzyme formation.

1. N-Terminal Tail

In cAPK, the N-terminal segment that precedes the conserved catalytic core is comprised of 39 residues plus a myristyl moiety that is attached co-translationally to the N-terminal glycine (Figure 6b). The first 10 residues of the catalytic subunit form a loop that folds the acyl group into an extended hydrophobic site. This site is comprised of multiple hydrophobic residues that originate from different parts of the protein. Phe-Pro-Phe (residues 100−102) are at the tip of the loop that links the C helix with β-strand 4. This loop, in contrast to the rest of the small lobe, is firmly anchored to the large lobe in all conformational states. The end of the conserved large lobe and the beginning of the C-terminal tail (residues 296−310) also contribute hydrophobic side chains to this hydrophobic pocket as does the E helix.[57] Thus, all parts of the molecule come together in this region.

Residues 10−30 constitute an amphipathic helix that docks via its hydrophobic surface to the large lobe. The helix ends with Trp30, which fits into a hydrophobic groove that is lined by Arg93 in the C helix of the small lobe and Arg190 that is part of β-strand 9 at the edge of the active site cleft in the large lobe.[58] Phe26 also fills a portion of this socket. The C-terminus of the A helix and the C-terminus of the conserved C helix in the small lobe meet at this point and serve to stabilize each other via the interactions of Glu96 in the C helix with the backbone amides of Lys29 and Ser34 at the end of the A

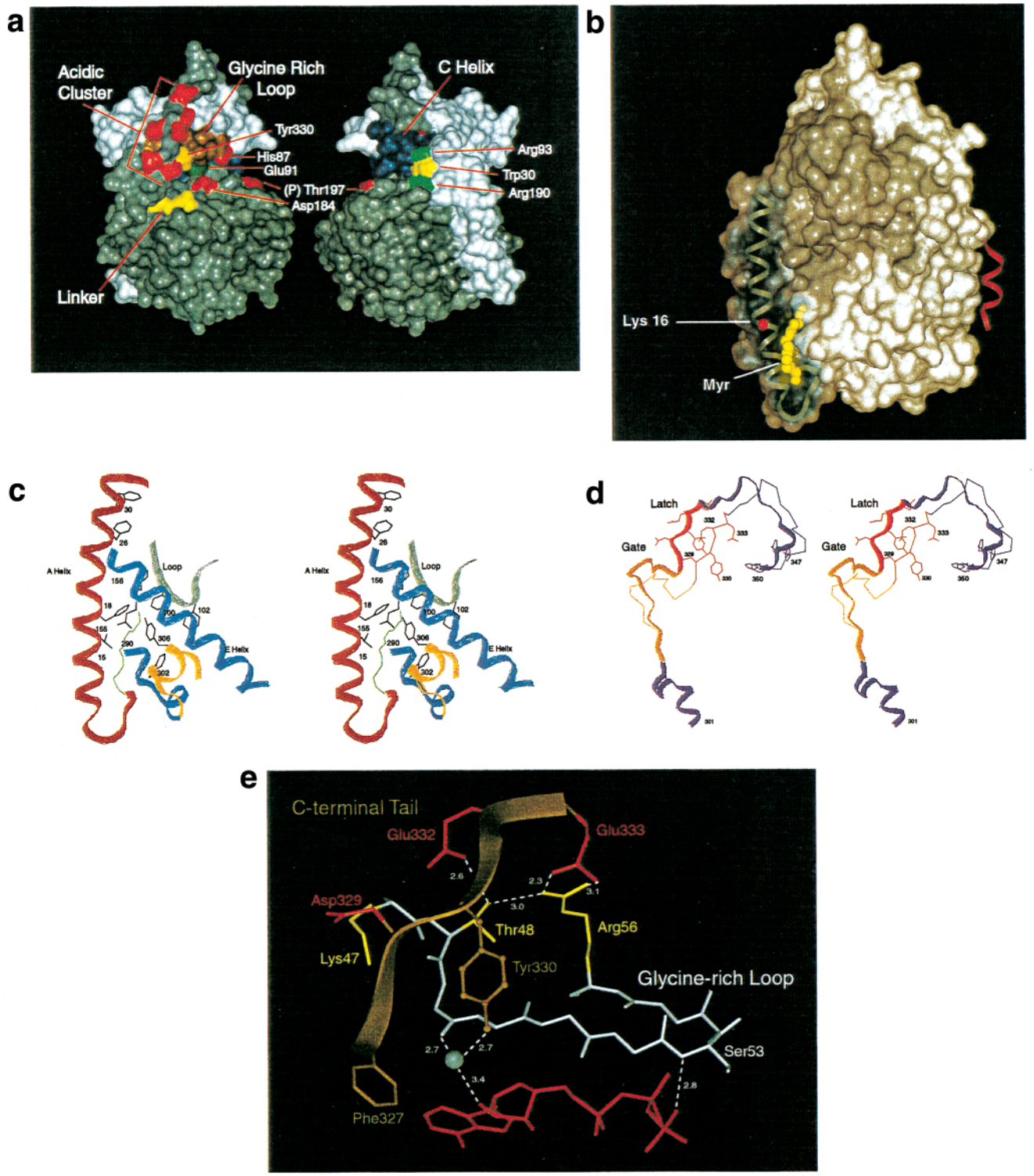

Figure 6. Carboxyl- and amino-terminal tails wrap around the conserved core of the catalytic subunit. (a) Space-filling model of the open mammalian catalytic subunit bound to PKI(5−24) (1CMK). In this diagram, PKI(5−24) has been deleted. The coloring of the active site cleft is the same as in Figure 2. Additionally, key residues in the "latch" in the C-terminal tail are highlighted. The "latch" is an acidic cluster comprised of Tyr330 (orange) and Asp328, Asp329, Glu331, Glu332, Glu333, and Glu334 (red). The view of the molecule rotated 180° is on the right. (b) Exposed A helix that is anchored to both lobes of the core. Lys16 where a cysteine was engineered and then modified with fluorescein is also indicated. (c) Close-up stereoview of the myristic acid nestled among a number of hydrophobic residues, which come from various parts of the protein. (d) Full view of the C-terminal tail (residues 301−350) for the open (ribbon, 1CMK) and closed (stick, 1ATP) conformations. The small lobe and the large lobe anchors shown in purple, the "gate" region is in gold (315−327), and the "latch" region is in red (328−334). (e) The C-terminal tail contacts with the glycine-rich loop are shown, as highlighted from molecular dynamics calculations.[46] The gray ball is an ordered water molecule through which Tyr330 networks into the active site. (c) and (d) have been adapted from Zheng et al.[57]

helix. The multiple interactions between the two helices are shown in Figure 7a.

There are some unusual features of this N-terminal region, and it is subject to various posttranslational

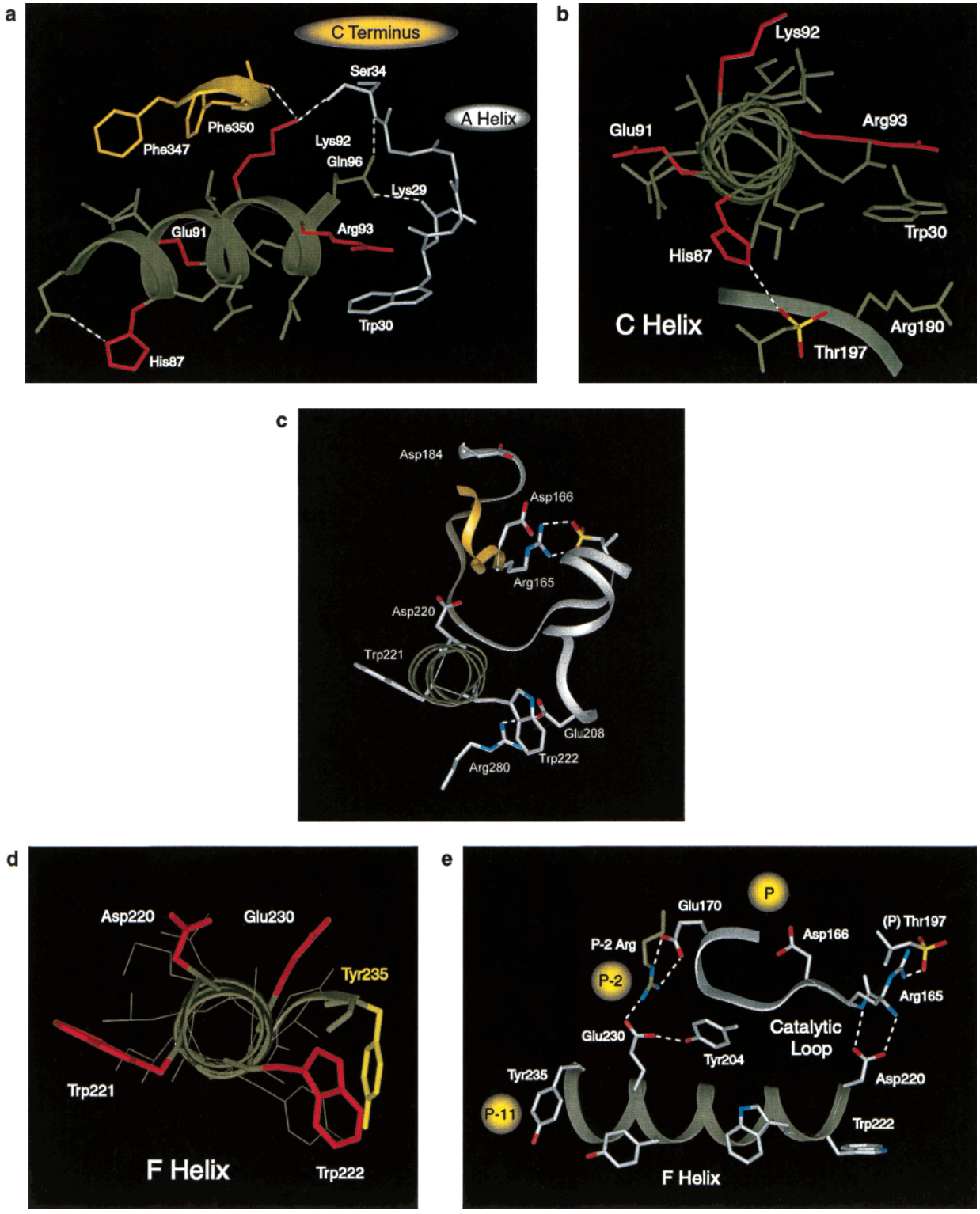

Figure 7. C helix, the activation loop, and the F helix are signal integration motifs. (a) View of the C helix showing key interactions with the activation loop, the C-terminal tail, and the A helix. (b) View of the C helix showing the interaction of His87 with phospho-Thr197 in the activation loop. This interaction only occurs in the closed conformation. Residues that contact different parts of the protein are shown in red. Specifically, Glu91 targets the active site, Lys92 helps to anchor the C-terminus, and Arg93 helps to anchor the N-terminal A helix. (c) Linkage of the F helix with the catalytic loop (gold) and the Glu208:Arg280 anchor. The two ion pairs Leu208:Arg280 and Arg165:Thr197 complete the circuit between the F helix and the activation segment (residues 184−208). (d) Residues from the F helix that contact various parts of the protein. Asp220 targets the active site, Trp221 is buried in the hydrophobic core of the protein, Trp222 helps to stabilize the Glu208:Arg280 ion pair, and Glu230 comprises the P-2 peptide-binding site. Tyr235 (yellow) goes to the P-11 peptide-binding pocket. (e) View of the F helix, showing its contributions to three peptide-binding subsites (P, P-2, and P-11).

modifications as well as myristylation. In the recombinant protein, which is not myristylated due to a lack of *N*-myristyl transferase in *E. coli*, the first 10−15 residues are disordered in the crystal structures.

Only in the structure of the mammalian porcine enzyme is the complete N-terminus including the myristyl moiety visible.[26] The myristyl moiety conveys enhanced thermostability to the catalytic subunit,[59] and the crystal structure of the mammalian myristylated protein defines the hydrophobic interactions between the N-terminus and the rest of the catalytic subunit. Fluorescence anisotropy,[60] as discussed later, also shows that the myristyl moiety stabilizes the N-terminus and has additionally provided insight into the dynamic feature of this segment.

The first 14 residues of the catalytic subunit constitute a classic myristylation motif.[61,62] The catalytic subunit was, in fact, the first protein shown to be myristylated.[63] This motif which includes not only the myristyl moiety but also basic amino acids is also found in other protein kinases such as *src* and is sufficient to target proteins to membranes.[64,65] Both the acyl group and several basic amino acids are requirements for membrane association. The role of the myristyl group in cAPK has always been intriguing, because under most circumstances the enzyme is quite soluble. Nevertheless, this motif alone is capable of associating with membranes as demonstrated by characterizing a myristylated peptide corresponding to the first 24 amino acids of the catalytic subunit and by generating chimeras of *src* and the catalytic subunit where only the N-termini were swapped.[66]

As discussed later (section II.D.1), recent time-resolved fluorescence anisotropy studies using a mutant catalytic subunit (Lys16Cys) confirmed that the N-terminus is more ordered and less mobile when the N-terminal Gly is myristylated but also suggested that the mobility of the N-terminus may vary in an isoform-specific manner when holoenzymes are formed.[60] Specifically, the mobility of the N-terminus was not affected when the myristylated catalytic subunit was associated with the RIα subunit. However, when the catalytic subunit was associated with the RIIα subunit, the N-terminus became very mobile.[60] The type II holoenzyme also showed a synergistic enhancement of its ability to associate with lipid vesicles. Thus, there may be a switch mechanism for the N-terminus of the catalytic subunit similar to what has been observed in the Ca^{2+}-dependent switch in recoverin.[67]

There are several other unusual features of the N-terminus, although the biological significance of these recent findings remains to be elucidated.[68] Two different forms of the Cα catalytic subunit are found in most mammalian cells. They can be separated by ion-exchange chromatography and resolved by native polyacrylamide gel electrophoresis.[69,70] When both isoforms were crystallized independently, one form showed an acylated N-terminus anchored to the large lobe of the core[57] while the other showed the N-terminus to be disordered similar to the crystal structures of the recombinant protein. Bossemeyer showed subsequently that deamidation of Asn2 accounts for the differences between the two proteins.[71,72] This deamidation is thought to take place posttranslationally and could amplify or diminish the myristylation switch similar to the role of calcium for recoverin.[67]

Ser10 is also an autophosphorylation site. This Ser can be phosphorylated in *E. coli* and in vitro;[73] however, only the form that is not deamidated can be autophosphorylated by cAPK.[70,71] The enzyme that is phosphorylated on Ser10 has not been isolated from mammalian cells. Thus, if phosphorylation at this site has a functional consequence, it is most likely a transient one. The mature enzyme isolated from mammalian cells is phosphorylated on Thr197 and Ser338; both of these phosphates are very stable.[28,74] Analysis of the hydrogen bonding in the mammalian enzyme shows that the A helix is stabilized or capped by residues 10−13 (Ser-Glu-Gln-Glu)[75] and phosphorylation at Ser10 would break this helix cap.[76] Thus, there are several mechanisms whereby the mobility or exposure of the N-terminus could be altered.

A peptide corresponding to the first 16 residues of the catalytic subunit was analyzed by several methods including circular dichroism and NMR. Acylation causes an increase in the helicity of the peptide, while the helix was destabilized by phosphorylation at Ser10. Deamidation of Asn2 had no effect on the helical properties of the peptide.

The N-terminus is also subject to alternative splicing. Three isoforms were originally identified: Cα [77], Cβ,[78] and Cγ.[79] Although the most sequence variability is in the N-terminal 40 residues, all are identical in length, have a myristylation motif at the N-terminus, contain a potential cAPK phosphorylation site at Ser10, and contain Asn at position 2. Cα is constitutive in all cells, Cβ is expressed in a tissue-specific manner but is predominant in brain,[80] and Cγ is found primarily in testes. The catalytic subunit also undergoes alternative splicing at the N-terminus. For the Cα catalytic subunit there is an alternatively spliced variant, Cαs, that is found in sperm.[81−83] All of these splice variants reported so far involve only the first exon corresponding to the first 16 residues. In Cαs, residues 1−14 of Cα are replaced with six new hydrophilic residues. Cαs does not have a myristylation motif. Thus, on the basis of size and physical properties, the N-terminus is unlikely to occupy the extended hydrophobic pocket filled by the myristylated moiety in the Cα subunit. For the Cβ subunit there are also several unique splice variants at the N-terminus.[84,85] Once again, these splice variants are associated exclusively with the first exon. At least four alternative splice variants exist, and none have a classic myristylation motif. The functional consequences of these variations at the N-terminus are not known; however, expression of a 1−14 deletion mutant of the Cα subunit suggests that this protein is less soluble when expressed in *E. coli*, is more thermolabile, but is kinetically indistinguishable from the longer Cα subunit.

The A helix serves to anchor the small lobe to the large lobe; in the absence of the A helix, the hinge between the small and large lobes would likely be much more flexible. The A helix also contributes to tethering of the C helix at its C-terminal end. This positioning of the C helix appears to be critical for

all protein kinases; however, the mechanism that each protein kinase uses to position the C helix is different. Figure 2 (right) shows the exposed outer surface of the C helix when only the core is present. In contrast, Figure 6a demonstrates how the C-terminus of the C helix is shielded by the A helix. The critical positioning of Trp30 by Arg93 and Arg190 is also highlighted clearly.[58] Replacement of Trp30 with Ala or Tyr introduces considerable thermoinstability.[58]

2. C-Terminal Tail

The C-terminal tail consists of 50 residues that wrap around the surface of both lobes (Figure 6d). The first 14 residues (residues 301−314) are firmly anchored to the large lobe and, as might be anticipated, do not undergo conformational changes. As seen in Figure 6c, these residues also provide part of the hydrophobic site where the N-terminal myristyl group docks. The last four residues, Phe-Thr-Glu-Phe, also are anchored to the catalytic core, but in this case they are docked to the small lobe.[56,86] The α-carboxyl group of Phe350, for example, forms a buried ion pair with the side chain of Lys 92 in the C helix. The hydrophobic side chains of Phe347 and Phe350 are buried in a hydrophobic pocket. Furthermore, replacement of Phe350 with Ala renders the enzyme inactive, while replacement of Phe347 with Ala yields a very unstable enzyme.[56] Ser338 is a stable site of phosphorylation which in some structures interacts with Lys342 and appears to stabilize the turn. Replacement of Ser338 with Ala destabilizes the enzyme.[73]

The remainder of the C-terminal tail can be quite flexible, and the degree of order is determined by ligands. Residues 315−327 fold over the adenine-binding pocket and form a "gate" that modulates access of ATP, while residues 328−334 are mostly acidic and probably help to draw basic substrate peptides or proteins to the active site cleft. In the midst of this acidic cluster is Tyr330, which contributes to the P-3 peptide recognition site in the ternary complex.[56,87] This P-3 site which serves to bind to the P-3 Arg in the peptide substrate and/or inhibitor is another site that is formed by residues coming from different parts of the protein. Glu127 at the end of the linker that joins the small and large domains also binds directly to the P-3 Arg. A stable water molecule also nucleates this site.[55] The C-terminal tail is also the site of cleavage by a highly specific kinase splitting membrane protease.[56]

On the basis of a comparison of various open and closed conformations, the C-terminal tail can be divided into four segments. The two ends, as discussed above, are anchored to each lobe and do not show significant conformational flexibility. The C-terminus of the catalytic subunit (Phe-Thr-Gly-Phe) was recently discovered to be a specific motif that is shared by several members of the AGC protein kinase family. This was isolated in a yeast two-hybrid screen as a binding partner for PDK1.[86] The hydrophobic binding pocket for this motif in the small lobe of the catalytic subunit was first described by Batkin et al.[56] Their mutational analysis demonstrated the importance of this site for the structure and function of the catalytic subunit, while the PDK1/PKC studies suggest that this motif can also contribute to cross-talk between heterologous protein kinases. The specific motif that occupies this discrete binding pocket further defines this site of anchoring.[86] The intervening sections, however, are quite flexible and highly sensitive to ligands. Residues 315−327 serve as a gate for access of the nucleotide.[43] This section folds over on top of the adenine ring once it is bound and helps to shield it from solvent. The following string of acidic residues surrounding Tyr330 is thought of as the "latch" to the gate whose principle role appears to be to attract basic peptides and position them for docking to the active site and to clamp down over the base of the glycine-rich loop. The dynamic properties of this tail are quite variable. In the ternary complex containing ATP or AMPPNP, PKI(5−24), and the catalytic subunit, the entire length of this segment is firmly anchored to the core. The charged segment snaps onto the small lobe making numerous contacts. The malleability of this segment was recognized long ago based on chemical modifications with sulfhydryl group reagents and carbodiimides that were protected in the presence of ATP and peptide and resistant to the kinase splitting membrane protease[88] and is reviewed by Batkin et al. [56] This has now been confirmed by many crystal structures. That the enzyme exists in a variety of conformational states is clear. Equilibrium strongly favors the closed state in the presence of ATP and peptide. In the open conformation the tail is not only opened but also more disordered. In some cases, the tail cannot be reasonably traced.

C. Signal Integration Motifs

The protein kinases have evolved into highly sophisticated molecules that are poised to receive and transmit transient signals. This is accomplished by an integrated network of intramolecular signaling that permeates to all parts of the molecule. The catalytic site does not simply rest on an inert scaffold; the scaffold itself is highly dynamic and linked by conserved motifs to the active site. This is in contrast, for example, to the tyrosine phosphatases where a small linear cassette contains all the essential components for catalysis. For example, the scaffold surrounding this phosphatase cassette is completely different in the *Yersinia* protein tyrosine phosphatase,[89] and in the cell cycle control phosphatase, cdc25,[90] even though the catalytic sites are virtually identical. For protein kinases, the entire molecule is focused on transferring the γ-phosphate of ATP; the surrounding scaffold is an integral part of catalysis. The extended network that mediates the integration of signaling in protein kinases was apparent from the sequence analysis even before the crystal structure provided a molecular framework for that integration.[22] It has only been reinforced by the many crystal structures that have emerged over the past decade.

The subdomains that contribute either directly or indirectly to catalysis can be divided into two general categories: those that contribute directly to catalysis and those that contribute indirectly to the signaling

network. We refer to the latter as signal integration motifs. These motifs are typically helices or loops and in general correspond to the sequence modules defined by Hanks.[2] The signal integration motifs in the core must have certain defined criteria. First, they must contain at least one conserved residue. Second, they must link in a nonlinear manner at least three different parts of the molecule (i.e., small lobe, large lobe, N-terminus, C-terminus, or an accessory protein). Third, they must touch at least one other conserved residue in a noncontiguous part of the protein. Fourth, these motifs must be able to influence catalysis even though they are far from the actual site of phosphoryl transfer. Typically, they do not directly touch the substrate.

The loops and helices that contribute to catalysis and signal integration in the catalytic subunit are summarized in Tables 3 and 4. The catalytic motifs that directly bind substrates and contribute to phosphoryl transfer line the active site cleft. They include the glycine-rich loop in the small lobe and the catalytic loop, the magnesium positioning loop, and the substrate positioning loop in the large lobe. In addition, there are at least three signal integration motifs that lie distal to the active site. These include the C helix in the small lobe and the activation loop and F helix in the large lobe.

The loops of catalysis, shown in Figures 3 and 5 and discussed earlier, are remarkable not only for the precise and connected way in which they poise the γ-phosphate of ATP for transfer but also in the ways that each motif reaches out to other parts of the molecule. In this section, we will focus on the three signal integration motifs: the C helix, the activation loop, and the F helix (Figure 7**)**. In addition, in the following section, we will consider the dynamics of two peripheral and nonconserved signal integration motifs: the A helix and the mobile C-terminal tail (residues 328−334). These motifs are not themselves conserved but the way in which they contribute to the signaling network is conserved.

1. C Helix

In the small lobe, there are two motifs that are integral for catalysis: the glycine-rich loop which contributes directly to catalysis and the C helix which contributes indirectly. The C helix is one of the most important signal integration motifs in the core. It is essential for signal integration in cAPK and most likely for all protein kinases. One turn alone of the C helix (residues 91−93) directly interacts with the active site, the N-terminus, and the C-terminus (Figure 7a and b). Glu91 interacts with Lys72 in β-strand 3 that positions the α- and β-phosphates of ATP. Lys92 forms a buried ion pair with the α-carboxylate of Phe350 at the C-terminus. Arg93 forms a wall of the pocket that locks Trp30 at the end of the A helix into its socket.[58] His87 in the preceding turn of the helix binds to phospho-Thr197 in the activation loop when the enzyme is in the active conformation. The precise position of this helix thus can be oriented in principle by many factors such as the phosphorylation state of the protein or nucleotide binding. The recent hydrogen/deuterium exchange studies of Anderson et al.[91] provide direct evidence that nucleotide (ADP) is sufficient to protect the C helix from deuterium exchange even though the C helix does not directly contact the nucleotide.

2. Activation Loop

In the large lobe, the activation loop and the F helix (Figure 7c−e) are signal integration motifs. Phosphorylation of Thr197 in the activation loop (Figure 5) organizes the enzyme globally into a conformation that is poised for catalysis or for inhibition. That single phosphate via its interactions with Lys189 and Arg165 organizes four functions: (1) catalysis, (2) peptide recognition, (3) anchoring of the A helix, and (4) inhibition by regulatory subunits. The phosphate is the central organizing moiety for all of these functions; however, proceeding the phosphate is a tryptophan, Trp196, which is essential for recognition of the R subunit. Although no structure of an R:C complex has yet been solved, it is likely that the regulatory subunits will dock to this region. β-Strand 9 is positioned by the phosphate. The opposite surface of β-strand 9, specifically Arg190, reaches out to position the A helix. The surface created by the C helix and β-strand 9 can also serve as a docking site for other proteins such as cyclin in the case of cdk2.[41] These two contiguous surfaces are poised to receive signals from other molecules or domains. In the case of the catalytic subunit, it is the N- and C-terminus that are positioned by this surface. As seen in Figure 5, Arg165, stabilized by the DFG loop (Figure 5, top right), is the central link for organization of the active site cleft.

3. F Helix

The extremely hydrophobic core of the large lobe has not yet been studied in detail, but a striking feature of the protein kinase core is its extreme hydrophobicity. The two buried helices that permeate the center, the E helix and F helix, are particularly intriguing. Helices in proteins are typically amphipathic with one hydrophobic surface facing inward and the other more hydrophilic surface facing the solvent. The E and F helices, in contrast, are striking in their overall hydrophobicity. They are flanked at each end by hydrophilic residues and one of these flanking segments is a classic signal integration motif. Residues 220−222 (Asp-Trp-Trp) are highly conserved with Asp220 being invariant. Asp220 buttresses the catalytic loop by hydrogen bonding to the backbone amides of Arg165 and Tyr164. Arg165 is a key residue in most protein kinases and is anchored to the activation loop when it is phosphorylated. Arg165 is thus a critical bridge to the active site. Trp222 is also conserved in most protein kinases. It appears to stabilize a relatively buried ion pair between Arg280 and Glu208. Glu208 lies at the end of the peptide positioning loop, while Arg280 is the farthest outlier in the set of conserved residues in the core. It lies between the H and I helices. This segment actually can be thought of as a "flap" that is anchored to the core by mostly hydrophobic interactions with the exception of the anchoring of Arg280 to Asp208. Scanning mutagenesis of the yeast cata-

lytic subunit of cAPK, tpkI, showed that mutation of either Asp208 or Arg 280 leads to reduced catalysis whereas mutation of both residues is compensatory.[92] The close proximity of these two residues was thus actually predicted prior to and independent of the solution of the X-ray structure.

D. Dynamics

Understanding the dynamic properties of the catalytic subunit and how those dynamic features correlate with catalysis is one of the most important questions although it is still largely unanswered. As indicated above, compelling evidence from many different directions indicates that the catalytic subunit is quite malleable and that opening and closing of the cleft, or at least opening and closing of the glycine-rich loop, is to some extent essential for catalysis. Phosphoryl transfer for the catalytic subunit is extremely fast, greater than 500 s^{-1}.[44] However, k_{cat} is only 20 s^{-1}. The rate-limiting step is release of ADP or more likely the conformational changes that allow for release of the nucleotide.[44,93−95] Achieving this release requires at least a partial opening or relaxation of the cleft. It should also be emphasized that the rate-limiting step may be different for other protein kinases.[96] The catalytic subunit is somewhat unusual in having a C-terminal tail that functions more-or-less as a gate that modulates access of nucleotide to the active site cleft by clamping down over the glycine-rich loop.

While crystallographic evidence defines several different conformations of the catalytic subunit, we are not yet able to directly measure opening and closing of the cleft in solution on a time scale that would correlate with catalysis and with the equilibrium states that exist within the cell.

1. Fluorescence Anisotropy

To evaluate conformational changes in solution requires methods other than crystallography, which provides only fixed snapshots of conformational diversity. Time-resolved fluorescence anisotropy (TRFA) is a method for measuring the rotational diffusion of fluorescent reporter groups. In combination with site-specific labeling, reporter groups can be introduced into specific solute accessible regions of proteins to monitor local backbone flexibility. Anisotropy measurements involve the selective electronic excitation of reporter groups whose absorption moments are aligned parallel to vertically polarized light. The time course of the emission depolarization of these reporter groups generally follows the randomization of the orientation of their emission moments within the excited-state lifetime and, thus, their rotational diffusion. Reporter groups conjugated to amino acid side chains undergo diffusional processes that would include complex sidearm (tether arm), local backbone, large-scale internal, and whole-body motions.

TFRA has been used to probe various sites in the catalytic and regulatory subunits of cAPK and has also been used to map the ordered and disordered regions of PKI. These proteins are excellent candidates for TRFA for several reasons. In the case of the catalytic subunit, there are only two endogenous cysteines and both can be protected against covalent modification by ATP. Replacement of either or both cysteines with Ala also does not influence activity. Thus, unique cysteines for covalent modification can be engineered into the protein. An initial set of surface sites was selected based on the crystal structure.[97] The crystal structures also provide an opportunity to correlate TRFA-dependent changes in conformation with temperature factors of the regulatory subunit. RIα has two disulfide-bonded cysteines in the N-terminal dimerization/docking (D/D) domain and two additional unreactive cysteines in cAMP-binding domain B. Thus, cysteines can also be readily introduced and selectively labeled with fluorescein. For RIα there is crystallographic data for the cAMP-binding domains but no high-resolution structural information yet for the long linker region. PKI has no endogenous cysteines, so it is also an excellent candidate for TRFA. The details of PKI and R will be discussed later.

Although TRFA does not permit atomic resolution of the diffusional processes discussed above, the relative rate/amplitude of the local backbone motions around the attachment sites of reporter groups can be estimated under certain circumstances. This appears to be possible when the rates of the various diffusional processes are well separated from one another and/or when the amplitude of the local backbone motions are very much larger than either the tether arm or internal motions. Support for this comes from the observation that the 'fast' rotational correlation time ($Ø_{fast}$) of fluorescein (FM) conjugated to five sites of cysteine substitution in the catalytic subunit is inversely correlated to the average main-chain atom temperature factors of the adjacent residues.[97] As seen in Figure 6e, Lys16 is located on the solvent-exposed surface of the A helix near the N-terminus. This site is associated with high-temperature factors and is near nonresolved residues in the crystallographic structure. N-Terminal myristylation of this protein, which stabilizes the N-terminus to the core catalytic domain, shifts the $Ø_{fast}$ value from 1.9 to 2.9 ns, a result that is consistent with the crystallographic observations.[97] For the myristylated catalytic subunit, this acyl group binds to a hydrophobic pocket on the surface of the large lobe. The first 12−15 residues are not visible in the crystal structures of the nonmyristylated recombinant enzyme. For nonmyristylated catalytic subunit, the $Ø_{fast}$ value at this site of cysteine substitution and FM labeling (Lys16Cys) near the weakly anchored N-terminus is 1.9 ns. Though not completely understood, in some circumstances the amplitude, but not the rotational correlation time, of the 'fast' anisotropy decay process appears to be a more sensitive measure of the local backbone flexibility around the sites of conjugation. This is the case for the fluorescein conjugated to three cysteine-substitution sites in PKI discussed below. N-Terminal myristylation of this protein, which stabilizes the N-terminus to the core catalytic domain, shifts the $Ø_{fast}$ value from 1.9 to 2.9 ns, a result that is consistent with the crystallographic observations.

2. Molecular Dynamic Simulations

While crystal structures have provided snapshots of the catalytic subunit in both open and closed conformations with different bound ligands, there still remains the question of how the specific conformational changes occur that allow for ATP binding and ADP release. Molecular dynamics simulations were performed with the "closed" structure (PDB code: 1ATP) to better understand how the concerted motions that allow for opening and closing of the cleft are mediated.[46] For these calculations ATP and PKI-(5−24) were removed in an effort to understand what motions would take place once the catalytic subunit was stripped of ligands. Four types of analyses were carried out. One identified rigid domains. Another identified correlated motions. A third method analyzed variations in dihedral angles to highlight regions of flexibility. A final method analyzed hydrogen-bonding frequency searching, in particular, for stable, nonlinear segments. As anticipated, two major domains were defined that correspond in general to the small and large lobes of the conserved core; however, several stable subdomains were also identified. The calculations also indicated nonlinear linkages between some of those subdomains.

Overall the most flexible part of the protein is the glycine-rich loop. This is the loop that is intimately involved in nucleotide binding with the tip of the loop, specifically the backbone amide of Ser53, thought to be essential for optimal phosphoryl transfer. This conclusion is not only consistent with the crystal structures, but also supported by extensive mutagenesis of the loop.[30−32]

Somewhat surprisingly, a very stable subdomain involving two nonlinear regions linked by hydrogen bonds was identified in the small lobe (Figure 6e). Specifically, Lys47 and Thr48 at the beginning of β-strand 1 and Arg56 at the end of β-strand 2 have a high frequency of hydrogen bonding to a segment in the C-terminal tail (residues 329−332). Lys47, Thr48, and Arg56 form the base of the glycine-rich loop. The segment at the C-terminus, Asp329, Glu332, and Glu333, is part of the "latch", described by Shaltiel,[55,56] that clamps the glycine-rich loop down on top of the substrate with the ring of Tyr330 forming a nodule that links the P-3 Arg in the peptide to the 3′OH of the ATP ribose ring and Glu127 at the boundary of the linker and the large domain. A stable water molecule helps to nucleate this site. The identification of this stable subdomain by the theoretical calculations, and in full agreement with extensive experimental evidence, provides a potential mechanism involving the C-terminal tail in opening and closing of the glycine-rich loop at the active site cleft.

Another unanticipated finding was the tracking of Asp184 when the correlated motions were calculated. Although Asp184 is part of the loop between β-strands 8 and 9 in the large lobe, it tracked conspicuously with the small lobe. As pointed out in Figure 3, this Asp plays a critical role in bridging the two domains. Asp184 binds to the activating magnesium ion that bridges the α- and β-phosphates of ATP and more than any other residue directs the γ-phosphate toward the peptide that is poised to receive it. Its striking linkage with the small domain further emphasizes the potential mechanistic importance of this residue.

In contrast to Asp184, which tracked with the small lobe, a portion of the small lobe was also found to track with the large lobe using a rigid-body extraction method. This segment is residues 98−105 that comprises the hydrophobic loop between the C helix and β-strand 4. The linkage of this segment with the large lobe was pointed out in Figure 6c. The tip of this loop, residues 100−102 (Phe-Pro-Phe), is a prominent part of the acyl pocket where the myristyl moiety docks.

A final conclusion was based on an analysis of the dihedral angles. This approach suggests that the domain movement of the small lobe relative to the large lobe is not achieved by simply rotating about a single hinge. In addition to the linker region, residues 120−126 (Met-Glu-Tyr-Val-Ala-Gly-Gly) which contribute to the opening of the cleft, other sites contribute such as residues Leu106 and Glu107 as well as Val98 and Asn99. These residues flank the hydrophobic loop, as discussed above, that is anchored to the large lobe.

These calculations have not been carried out yet on other protein kinases, but it will be interesting to see if similar results are obtained with regard to the glycine-rich loop, Asp184, and the opening of the cleft. The glycine-rich loop and Asp184 are invariant features of all protein kinases, and the role that each plays in catalysis and movements at the active site cleft is thus likely to be conserved.

III. Inhibitors of the Catalytic Subunit

Unlike many protein kinases whose activity is regulated by the transient addition of a phosphate to the activation loop, cAPK is assembled as a fully active enzyme that is kept in its inactive state by inhibitory proteins. There are two classes of inhibitors; both bind with high affinity (0.2 nM) and are highly specific for the catalytic subunit. These are the heat-stable protein kinase inhibitors (PKIs) and the regulatory (R) subunits. Unlike the intensely concerted catalytic subunit whose sole function is phosphoryl transfer, the inhibitor proteins are heat-stable, modular, and multifunctional proteins. In addition, they are structurally very dynamic; both show major regions of disorder as well as globular domains and/or regions of well-defined secondary structure. This is in striking contrast to the more subtle conformational changes that the catalytic subunit undergoes. Unlike the catalytic subunit which is a globular protein with a well-integrated and finely tuned network that links most parts of the protein, the functional modules of PKI and R are more segregated and uncoupled.

A. Protein Kinase Inhibitor

PKI is a small heat-stable protein that is mostly disordered in solution.[17,98] It is also a multifunctional protein. It harbors a highly specific high-affinity binding site for the catalytic subunit near its N-

terminus[99,100] and a nuclear export signal (NES) near its C-terminus.[18] While many questions remain about the physiological role of PKI, it is an excellent example of a multifunctional modular regulatory protein. It was first discovered as a contaminant that co-purified with the catalytic subunit.[101] There are several isoforms[102] that are expressed in a tissue-specific manner including prominent expression in the brain. It is also expressed in a cell-cycle-specific manner.[103,104]

Like the regulatory subunits, PKI binds with high affinity to the catalytic subunit and thus provides a highly specific biological mechanism for inhibiting catalytic activity in the presence of cAMP.[17] PKI has a pseudosubstrate consensus sequence where the P site is an Ala rather than a Ser or Thr. In addition, formation of a high-affinity complex with catalytic subunit requires ATP.[105,106] ATP has a K_m of 10 μM for catalysis but binds to the C:PKI complex with a K_d of 60 nM. Alone, PKI has a K_D of 230 nM, whereas in the presence of ATP the K_i is 0.2 nM.[107] High-affinity binding of PKI and ATP also requires more than one metal ion.[108] Thus, there are several levels of cAPK regulation involving PKI. Whether all are important physiologically is unclear. For the purposes of this review, we will focus on the biophysical properties of PKI.

The inhibitory properties of PKI are localized at the N-terminus[99,100] and were mapped comprehensively by Walsh and Glass.[17] The importance of the arginines at the P-2, P-3, and P-6 positions, as well as the P-11 Phe, for high-affinity binding to the catalytic subunit was established well before a crystal structure of the complex was solved. Identification of this high-affinity peptide inhibitor certainly facilitated the first structural solution of a binary complex with PKI(5−24),[20] and the crystal structures have unambiguously confirmed all of the elegant peptide studies that preceded the structure solution of the catalytic subunit.[20]

The NES at the C-terminus of PKI was discovered relatively recently[18] and provides a mechanism for rapidly exporting the catalytic subunit from the nucleus. On the basis of NMR,[98,109,110] circular dichroism,[111−113] and time-resolved fluorescence anisotropy,[114] PKI appears to be mostly disordered in solution. As indicated in Figure 8 (top), there are only two small ordered regions, both helical. One helix at the N-terminus, residues 1−12, overlaps with the inhibitor sequence. It is the hydrophobic surface of this amphipathic helix, with the P-11 Phe being a major determinant, that binds to a hydrophobic site on the surface of the catalytic subunit and provides the peripheral binding site that is essential for high-affinity binding.

The segment that follows contains the arginine-rich consensus sequence that docks to the active site cleft of the catalytic subunit. As predicted by Cheng[115] and Scott,[99] P-6, P-3, and P-2 arginines as well as the P+1 Ile are the primary determinants for binding to the active site cleft. This region only assumes order upon binding to the catalytic subunit; in solution, it is disordered (Figure 8, bottom). The importance of this plasticity is unclear, but it seems to occur frequently

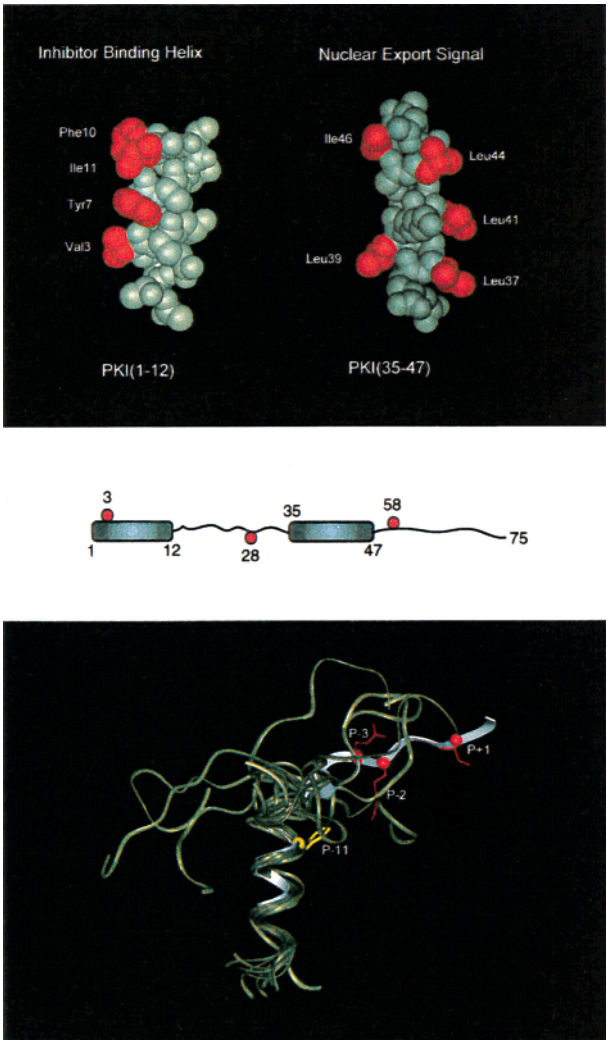

Figure 8. Protein kinase inhibitor (PKI). The top panel shows helix 1 (residues 1−12) and helix 2 (residues 35−47) of PKI. This figure was adapted from Hauer et al.[98] Hydrophobic residues are shown in red. In helix 1, the hydrophobic residues are involved in binding to the catalytic subunit. For helix 2, Leu37, Leu41, Leu44, and Ile46, but not Leu39, are essential for nuclear export.[18] Helix 2 overlaps with the NES. The structural organization of the heat-stable protein kinase inhibitor, shown in the middle, includes only two regions of ordered secondary structure. The red dots correspond to sites where cysteines were introduced and then labeled with fluorescein. Shown below, in tan, is the ensemble of structures (residues 1−24) seen with NMR. The white ribbon corresponds to the conformation of PKI(5−24) when it is bound to the catalytic subunit.

in protein kinase regulatory proteins. Presumably, long-distance electrostatic interactions initially draw PKI, as well as basic substrates, to the active site of the catalytic subunit. The kinetic, substrate specificity, and structural economic advantages of having a flexible basic segment that contributes to drawing peptides to the active site of the catalytic subunit have not been rigorously addressed; however, phosphorylation sites are often located in flexible loops or at the C- or N-terminus of proteins. Flexible motifs also provide structural economy; no stable scaffold is required to present the recognition motif.

The second small region of order in PKI is another amphipathic helix that overlaps with at the NES (Figure 8, top). Mutational analysis demonstrated

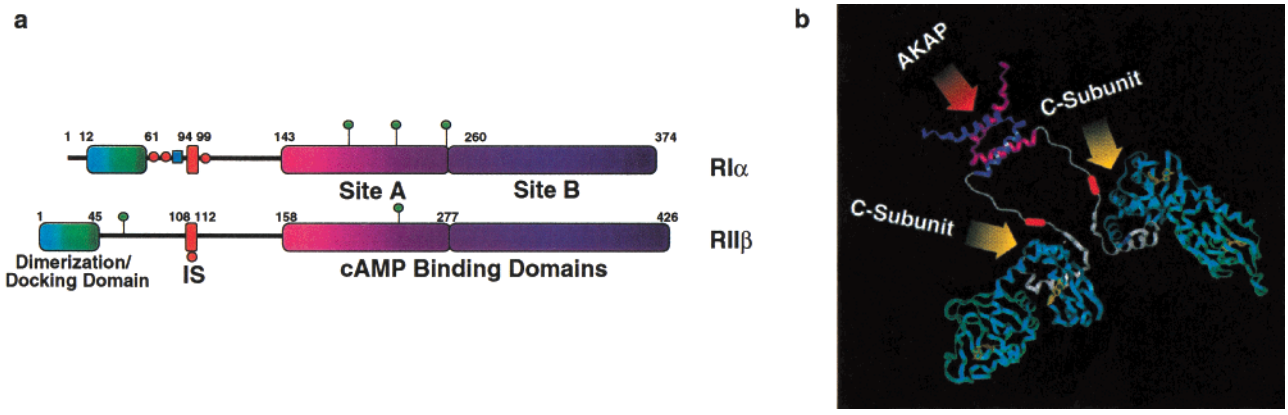

Figure 9. Organization of the regulatory subunits. (a) Schematic domain organization of RIα and RII*β*. Green circles indicate endogenous tryptophans. Red circles indicate heterologous and autophosphorylation sites. The green box is the proline-rich region. IS is the inhibitory sequence. (b) Structural organization of the regulatory subunit where the two stable domains (the D/D domain at the N-terminus and the cAMP-binding domain at the C-terminus) are joined by a disordered and flexible linker. The cAMP-binding domains are from RIα;[140] the D/D domain is from RIIα[142] (PBD code 1R2A). The red oval bars indicate the consensus inhibitor site. Binding sites for the catalytic subunit and for AKAPs are indicated by yellow and red arrows, respectively. This prototype of stable domains joined by disordered segments is likely to be common for many signaling proteins.

that the hydrophobic residues on the hydrophobic surface of this helix, but not Leu39, are essential for NES function.[18] No structures of an NES complexed with its binding partner have yet been solved.

The plasticity of PKI was demonstrated in solution by time-resolved fluorescence anisotropy.[114] Single cysteine residues were engineered at three specific sites: Val3Cys, Ser28Cys, and Ser58Cys. Each Cys mutant was then labeled with fluorescein 5-iodoacedamide. In the absence of the catalytic subunit, each of these positions was quite flexible as evidenced by the high amplitudes of the 'fast' rotational correlation times. When PKI was bound to the catalytic subunit, the two N-terminal sites became much less mobile. The amplitudes of 'fast' rotational correlation times at Val3Cys and Ser28Cys decreased 32% and 68%, respectively. The amplitude of the 'fast' rotational correlation time of the conjugated Ser58Cys mutant, however, was unchanged upon binding to the catalytic subunit, indicating that this region, which flanks the NES, remains relatively unstructured even when PKI is bound to the catalytic subunit. High-resolution NMR studies using [N^{15}]-PKI have confirmed this disorder−order transition.[98] This is an example of a protein-induced conformational change going from disorder to order. It is in contrast to the RII subunit-induced order−disorder transition that was observed for the myristylated N-terminus of the catalytic subunit.

B. Regulatory Subunits

Like PKI, the regulatory subunits are modular, multifunctional, and very stable.[6] Although there are different isoforms,[116−121] all show a common domain organization as summarized in Figure 9a. At the N-terminus is a D/D domain that not only maintains the protomer as a dimer, but also provides an anchoring surface on which the AKAPs dock. This is followed by a linker region that contains an inhibitor site that resembles a peptide substrate and is thought to dock to the active site cleft of the catalytic subunit. The linker regions contain multiple phosphorylation sites including an autophosphorylation site;[122−125] there is also a site for ubiquitination.[126] At the C-terminus are two tandem cAMP-binding domains. As discussed later, the linker, in contrast to the stable domains at the N- and C-termini, is disordered **(**Figure 9b**)**.

Activation of cAPK by cAMP is a highly cooperative process (Hill coefficient 1.3−1.5). That cooperativity is compromised when the D/D domain is deleted [127] and also when cAMP-binding domain B is deleted.[12] In the holoenzyme, cAMP-binding site B is accessible and first to bind cAMP. This causes a conformational change that opens up cAMP-binding site A. Binding to site A subsequently leads to the release of catalytic subunit.[127−129] The A domain is central in this activation process. It competes for either cAMP or the catalytic subunit.[130,131]

The docking of PKI and the R subunits to the catalytic subunit requires at least two sites to achieve high-affinity binding. All share a consensus site inhibitor peptide sequence that docks to the active site cleft of the catalytic subunit. This site resembles a peptide substrate, thus allowing the inhibitor proteins to serve as competitive inhibitors. In addition, each inhibitor has a peripheral recognition site that confers high affinity. For PKI, high-affinity binding is achieved by the contiguous amphipathic helix that lies N-terminal to the inhibitor site. The docking of PKI (5−24) to the catalytic subunit is shown in Figure 10; the hydrophobic site where the amphipathic helix docks is shown as well. The P-11 site is comprised of Tyr235 through Phe239 and Arg133. Rotating the molecule 180° reveals the major surface that binds the R subunit. This site was first identified as a docking site for the R subunit by scanning mutagenesis of tpk1, the yeast catalytic subunit.[132,133] Nonregulated phenotypes, identified in mammalian cells, showed the importance of His87 and Trp196.[134] This surface, required for high-affinity binding of the catalytic subunit, is comprised of basic residues that cluster around the phosphorylation site, Thr197, in the activation loop.[133,135,136] Trp196 is also

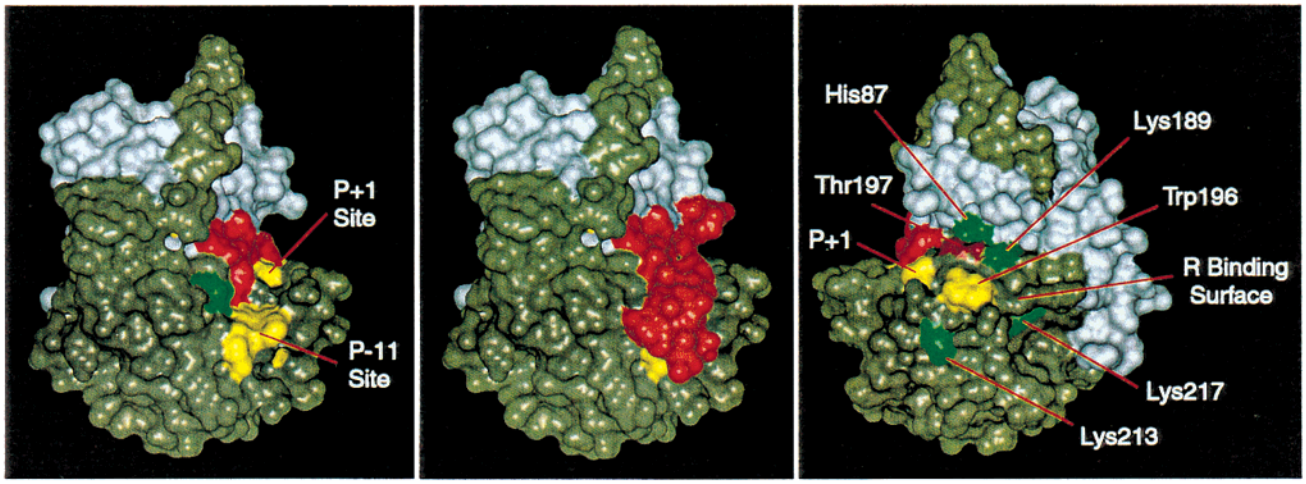

Figure 10. Distinct peripheral binding sites are required for high-affinity binding of R and PKI. The middle figure shows the ternary complex (1ATP) of the catalytic subunit bound to PKI(5−24) (red). The small lobe including the linker (residues 15−127) is shown in white; the large lobe including the C-terminal tail (residues 128−350) is shown in tan. On the left and on the right are two views of the catalytic subunit showing only the consensus inhibitor peptide filling the P-3 to P+1 pocket. On the left, the hydrophobic P-11 binding site (Tyr235-Phe239) and the hydrophobic P+1 peptide-binding site (Leu198, Pro202, Leu205) are shown in yellow and Arg133 is in green. The P-11 site, peripheral recognition site 1, is required for high-affinity binding of PKI. On the right, the molecule has been rotated 180°. The site required for high-affinity binding of the regulatory subunits, peripheral recognition site 2, is the surface surrounding Thr197 (dark red). It includes Trp196 (yellow) and Lys 213, Lys 217, and His 87 (green).

important for binding of the regulatory subunits.[136] The region of the RIα subunit that docks to this surface has also been mapped. Unlike PKI, these sites are not contiguous with the consensus inhibitor sites. Instead, they are localized primarily to cAMP-binding domain A.[136,137]

There are two general classes of R subunit isoforms (RI and RII).[118,119] The RI subunits have an alanine at the phosphoacceptor site in the consensus recognition sequence and, like PKI, require ATP for high-affinity binding. The RII subunits, on the other hand, have a phosphorylatable Ser in their consensus recognition sequence, and this site is autophosphorylated in the holoenzyme complex. Both R subunits are aligned as antiparallel monomers to form a homodimer. The RI subunits have two disulfide bonds that connect the antiparallel monomers in the homodimer configuration, [138,139] while the RII subunits have no covalent bonds connecting the monomeric elements of the homodimer. Though a structure of a full-length regulatory subunit has not yet been solved, the molecular details of the domains have been revealed by crystal structure solutions of the cAMP-binding domains of RIα[140] and RIIβ[131] and by the NMR-structure solutions of the dimerization/docking domain of RIIα.[141,142]

1. cAMP-Binding Domains

Like calcium, cAMP is an ancient signaling molecule. The cyclic nucleotide-binding (CNB) domain to which it docks is a highly conserved signaling module that is present in all organisms and conserved from bacteria to man. It is this module that allows the second messenger, cAMP, to mediate biological responses. The generation of cAMP is a primary stress response to glucose deprivation across the evolutionary spectrum, but in man, cAMP also mediates a diverse array of other signaling responses critical for development, metabolism, memory, ion channel modulation, and cell-cycle progression to name only a few. The cAMP-binding domain is conserved in all cases, although the partner protein or domain to which it is linked varies. In bacteria, the CNB domain is linked to a DNA-binding domain in the catabolite gene activator protein (CAP), where it mediates gene transcription from the lac promoter in the absence of glucose.[138] In mammals, the CNB domain is linked to protein kinases[138,143,144] as well as to phosphodiesterases, ion-gated channels,[145,146] and guanine nucleotide exchange factors.[147,148] In the case of cAPK, the cAMP-binding regulatory subunits are separate proteins that associate with the catalytic subunit and inhibit its activity in the absence of cAMP. For cGMP-dependent protein kinase, the closest homologue of cAPK, the regulatory and catalytic components are part of the same protein.[121]

Structures of the monomeric cAMP-binding domains have now been solved for two R subunit isoforms, (Δ1−91)RIα[140] and(Δ1−99)RIIβ.[131] These structures, in addition to the CAP structure,[138] allow us to deduce some general features of this domain. First is the highly conserved cyclic nucleotide-binding cassette that lies in the center of an 8-stranded β-barrel.[131,143,144,149] This forms the base of a "basket" where the cyclic phosphate moiety docks and is shielded from attack by phosphodiesterases. This cassette serves as a "motif" for identifying the domain and can be used readily to establish the phylogenetic lineage of this family. The cassette, shown in Figure 11 (bottom), is comprised of β-strand 6, a short P helix, a loop, and β-strand 7. Hallmarks of this motif are a conserved Glu (E200 and E321 in RIα and E221 and E332 in RIIβ) that binds to the 2′OH of the ribose and a conserved Arg (R209 and R233 in RIα and R230 and R341 in RIIβ) that lies buried at the bottom of the basket and binds to the cyclic phosphate. The

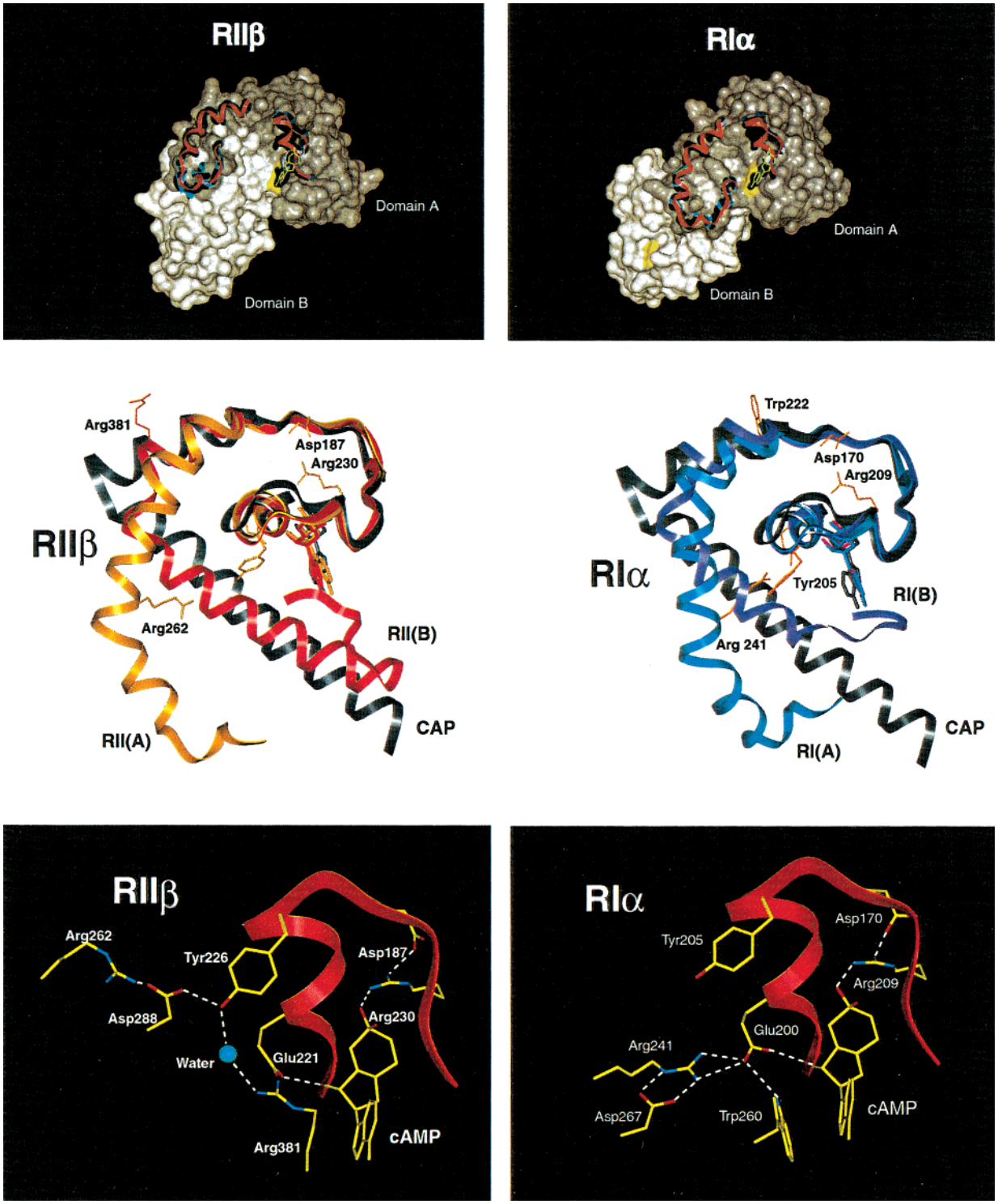

Figure 11. RIIβ and RIα structures. The top figures are the surface-rendered models for the RIIβ (1CX4, PDB code) and RIα (1RGS, PDB code) crystal structures. Shown in red are the C helices and the phosphate-binding cassettes. These two pictures highlight the different and isoform-dependent orientations of the cAMP-binding domains. cAMP is yellow. Domain A is tan, and domain B is white. In the middle panel are the ribbon diagrams of the phosphate-binding cassettes, through the C helix, superimposed with CAP. The RIIβ A and B domains are on the left, and the RIα A and B domains are on the right. The bottom panel shows a close-up view of a portion of the phosphate-binding cassette. Some of the important interactions for cAMP binding are highlighted. This includes residues that face the cleft interface and mediate the signal between the A domain and the B domain and the catalytic subunit binding site.

hydrophobic environment provided by the rest of the basket further shields the buried phosphate from solvent.

The phosphate-binding cassette (PBC) is surrounded by an 8-stranded β-barrel that is flanked by two helices. The two helices (αA at the N-terminus and αB at the C-terminus), by stacking against one another, anchor the β-barrel. αB is attached to an additional helix (αC); however, as seen in Figure 11 (top and middle), the position and shape of this helix vary between domains and are isoform-specific. This helix provides the "lid" for the basket and in the A

domain is structurally positioned by the B domain. The C helix of domain A, plus the B domain to which it is anchored by hydrophobic interactions, provides a solvent-rich domain interface that caps cAMP bound to domain A. This helix switches between at least two conformational states: the cAMP-bound state and the holoenzyme state when cAMP is released and catalytic subunit is bound. The critical positioning of this segment between cAMP-binding site A and the surface that has been identified as a catalytic subunit docking site by peptide mapping and by limited proteolysis allows it to serve as a potential switch.[135−137] So far, we only have structures of cAMP-bound conformations so we do not know the specific conformational changes that are associated with the binding of catalytic subunit and the release of cAMP. Several lines of evidence suggest, however, that the regulatory subunit undergoes a major conformational change upon shifting from the cAMP- to the catalytic subunit-bound configuration.

Within each cAMP-binding domain the loop between β-strand 4 and 5 is the most sequence variable. It consistently has high-temperature factors in all of the crystal structures, and in the B domain of RIIβ, the entire loop cannot even be traced.[131] This is also a major region of variability in both sequence and size between RI and RII isoforms where the RII subunits typically have a larger loop.[149] Proteolytic studies of RIIα indicate the β4-β5 loop in RIIα can be cleaved by proteases in the holoenzyme but is protected in the free R subunit.[150]

Unfolding studies in the presence of denaturants provide evidence as to the stability of this domain. On the basis of urea denaturation of RIα[151] and on point mutations and deletion mutants of RIα,[152,153] both in the presence and absence of cAMP, the A domain is very stable in the presence of cAMP. Unfolding is also highly cooperative. In the absence of cAMP, T_m is lowered from 5.1 to 3.5 M urea and the cooperativity is lost. Replacing the essential Arg209 in the phosphate-binding cassette with Lys causes the domain to behave in a manner that is equivalent to stripping away the cAMP.[130,153]

2. Overall Structure and Dynamics

The combination of site-directed labeling (SDL) and time-resolved fluorescence anisotropy (TRFA) have provided a mechanism not only for mapping domain boundaries in the RIα subunit but also for establishing cross-talk between the stable domains at the termini and the flexible linker. As indicated earlier, the RIα subunit is ideal for SDL/TRFA because two of its four cysteines are disulfide bonded and the remaining two are nonreactive. A set of unique cysteines were thus engineered throughout the molecule.[154] Labeling of sites in the linker region confirmed quantitatively for the first time the extensive mobility of this segment in the absence of the catalytic subunit. Thus, like PKI, the regulatory subunits display significant regions of plasticity that become ordered only upon binding to the catalytic subunit.

SDL/TRFA also provided a mechanism for further dissecting the linker region. By labeling a variety of sites, it was possible to identify regions that appear to be constitutively mobile; at the same time, the region that is masked by the catalytic subunit has been extended beyond previous predictions. On the basis of SDL/TFRA, residues immediately flanking the D/D domain (Thr6Cys and Leu65Cys) are highly flexible in the free RIα subunit and probably do not strongly interact with other structural elements. In contrast, sites of SDL/TRFA analysis more C-terminal to the D/D domain (Ser75Cys, Ser81Cys, and Ser99Cys) indicate less backbone flexibility particularly around Ser75Cys and Ser99Cys and suggest a weak interaction with a structured domain, probably the cAMP-binding domains.[154] Together, these results point to the existence of a short, flexible segment immediately flanking the C-terminal side of the structured D/D domain that could allow the interdomain and cAMP-binding region to pivot about the D/D domain. This interpretation is consistent with small-angle scattering results that suggest the existence of hinge movements at each end of the RIIβ subunit D/D domain.[155] Interestingly, this hinge region appears to be equally flexible whether cAMP, C subunit, or an AKAP fragment are bound since these agents have no effect on the backbone flexibility around the Leu66Cys site of mutation and fluorescein conjugation.[154] The mobility afforded by this arrangement could increase the rate of phosphorylation of adjacent membrane-associated targets of the AKAP-anchored holoenzyme.

The consensus recognition sequence within the interdomain linker, as discussed earlier, appears to be weakly associated with the tandem cAMP-binding domains in the open configuration, which may facilitate its ability to slip into the active site cleft of the catalytic subunit to inhibit its phosphoryl transferase activity. The binding of the catalytic subunit to the R homodimer and, thus, the formation of holoenzyme is associated with a dramatic decrease in the flexibility of a significant portion of the interdomain region including Ser75Cys and Ser81Cys. This suggests that the catalytic subunit-binding surface for the R subunit includes not only the consensus recognition sequence and part of cAMP-binding domain A, but also a 16+-residue segment N-terminal to the consensus recognition sequence. This extended region of protection by the regulatory subunit was also confirmed independently by chemical footprinting.[156]

Focusing on the tandem cAMP-binding domains, the main-chain atom temperature factors of the cAMP-bound (Δ1−91)RIα subunit[140] indicate that the N-terminal cAMP-binding domain A is more ordered (lower temperature factors) than the C-terminal cAMP-binding domain B. Moreover, two lines of evidence suggest that cAMP binding decreases the flexibility of both cAMP-binding domains. First, cAMP raises the concentration of urea required for chaotropic denaturation, indicating that cAMP stabilizes all or part of the R subunit.[151] Second, cAMP reduces the backbone flexibility around two sites of cysteine substitution and fluorescein conjugation in the cAMP-binding domains. One site (Ser145Cys) is far removed from the cAMP-binding pocket in domain

A; the other site (Ser373Cys) is adjacent to the cAMP-binding pocket in domain B.[154] The fact that cAMP binding to domain A reduces the backbone flexibility of a site ~26 Å away points to a 'tight' coupling of the low-nanosecond fluctuations and confirms that the A and B cAMP-binding domains are likely to be conformationally linked.

It is noteworthy that the character of the probable interaction between the interdomain and the tandem cAMP-binding domains changes with cAMP binding. This is observed as cAMP-induced changes in the emission decay kinetics (amplitude and lifetime) of conjugated fluorescein attached to the side chains of substituted cysteines along the interdomain (Leu66Cys, Ser81Cys, and Ser99Cys7) but not as a change in the fast anisotropy decay around the SDL/TRFA sites examined. This, again, points to an interaction between the interdomain and the cAMP-binding domains that is too weak for a 'tight coupling' of the backbone fluctuations between these two domains.

The probable association of the interdomain from, at least, Ser75 to Ser99 with the cAMP-binding domains is consistent with the observation that deletion of the first 91 residues of the RIα subunit produces a 100-fold increase in the rate of inhibition of the catalytic subunit catalytic activity by cAMP-bound RI subunit.[127] This 100-fold enhancement of the rate of inhibition would occur if the inhibitory sequence was anchored to the cAMP-binding domains by a segment of the interdomain creating steric hindrance for the catalytic subunit access. Deletion of the N-terminal 91 residues frees the inhibitory sequence resulting in enhanced accessibility for catalytic subunit binding.

IV. A-Kinase Anchoring Proteins

Initially cAPK was thought to be a relatively simple protein kinase whose activity was regulated solely by cAMP. Soluble and membrane-bound forms of cAPK were identified,[157,158] and the microtubule-associated protein 2 (MAP2) was shown early on to bind to the type II regulatory subunit of cAPK.[159] However, the concept of specific and widespread targeting of cAPK to unique sites in the cell is more recent. We now recognize not only that targeting is a major general mechanism for fine-tuning regulation,[160] but also that there is a large family of A-kinase anchoring proteins (AKAPs) that bind specifically to the N-terminal D/D domain of both RI and RII. [14−16,161] The binding is high affinity, typically 1−2 nM for RII and 50−300 nM and higher for RI.[162] The AKAPs, in general, have a targeting motif that directs the kinase to a specific subcellular location. The kinase-binding domain or motif often consists of a single amphipathic helix.[163]

A structural framework for the targeting of cAPK was provided by the recent NMR structure solution of the D/D domain of RIIα.[142] This X-type helix bundle is formed by the antiparallel alignment of the two protomers. The helix bundle provides a surface on which the AKAP helix docks. The structure is completely consistent with Ala scanning and mapping of residues important for AKAP binding. A structure of the RIIα D/D domain bound to the amphipathic R binding helix of Ht31 and AKAP79 provides for the first time a complete molecular framework for this docking motif.[141] We know nothing yet about the dynamic properties of the AKAPs. They appear to be modular and often serve as a scaffold for the assembly of several different signaling molecules.[14−16]

The AKAPs provide a new dimension to signal integration by cAPK. These scaffolds now establish cAPK as part of a large molecular machine where many regulatory enzymes can be localized at the same site.[164] Evidence is accumulating rapidly to show that AKAP-mediated targeting is essential for biological function.[165−167] Whether targeting is constitutive or dynamic remains to be established and most likely will vary with each AKAP and with the R subunit isoforms. However, it is this level of cell dynamics which will undoubtedly be the most challenging in the immediate future. Understanding these dynamic movements in the cell will require fluorescent techniques. In addition to labeled proteins, we increasingly rely on green fluorescent proteins (GFPs) where the fusion proteins have intrinsic fluorescence. The adaptation of blue fluorescent protein (BFP) and yellow fluorescent protein (YFP) partners where energy transfer is cyclic nucleotide-dependent offers an exciting window to explore this next level of complexity.[168,169]

V. Future Directions and Challenges

Although cAPK is one of the simplest and best understood members of the protein kinase family, there is still much to be learned about the structural dynamics of cAPK and its interactions with proteins such as PKI and the AKAPs. Particular challenges will be to understand the functional and structural consequences of the molecular complexes that are assembled by the AKAPs. Superimposed on this is the added level of complexity that is introduced by the multiple isoforms of both the regulatory and catalytic subunits.

A high-resolution crystal structure of any protein is an essential starting point; however, it is not adequate for defining the molecular events associated with catalysis, inhibition, and targeting. Technically our challenges will be to develop solution methods in parallel with crystallography that will allow us to observe the dynamic features of these proteins both at high resolution and in the time scales that correlate with functional parameters. Fortunately, there are many structural methods that have not been fully exploited that could yield valuable information regarding the structural behavior of cAPK in solution, and, in addition, major new advances have been made in many key areas.

A. Small-Angle Scattering

One promising structural technique is small-angle scattering, an analytical technique that can provide size and shape information of proteins. In the typical scattering experiment, an intense X-ray or neutron beam is focused on a protein sample in solution. The

protein's electrons scatter a portion of the incident flux, and the intensity of scattered radiation is measured as a function of the scattering angle. Many protein kinases and protein kinase complexes are too large to be analyzed by NMR and too inherently flexible to be analyzed by X-ray crystallography. Although small-angle scattering does not provide atomic resolution structural information, it can detect rather subtle changes in size or shape that might occur with ligand binding and with protein−protein interactions. With extremely bright sources of X-rays, such as synchrotron sources, it is even possible to monitor structural changes occurring with a time resolution of tens of milliseconds. If one of the components of a multisubunit complex can be expressed as a perdeuterated protein, neutron scattering can be used to determine the relative position of that protein in the complex. Changes in the relative positions of deuterated and proteated subunits in a complex can then be followed as concentrations of ligands and effectors are varied.

Small-angle X-ray and neutron scattering have been used already to study the type II cAPK holoenzyme complex and the data used to develop low-resolution 3D structural models.[155] The model developed for the cAPK holoenzyme is an extended dumbbell shape. Neutron scattering using holoenzyme prepared with protiated C and deuterated R indicated that each lobe of the dumbbell consists of the cAMP-binding domain of one R subunit and a catalytic subunit. Small-angle scattering studies with (Δ1−91)RIα:C dimer using deuterated (Δ1−91)RIα indicated that the catalytic subunit has a closed conformation in the RC dimer. By combining these small-angle scattering data with data from X-ray crystallography, site-directed mutation studies, and antipeptide antibody studies, relatively detailed quaternary structural models for cAPK can be developed. These models will be useful in understanding and designing site-directed mutagenesis experiments and can be refined as additional biochemical and biophysical data are obtained.

Small-angle scattering also has the potential to provide insights into the differences in structural and dynamic properties between RI and RII isoforms. Though the two isoforms of R are homologous, the regions between the dimerization/docking domain and pseudosubstrate domain are highly divergent in their sequences. It has been suggested that this region may be more rigid in RI than RII isoforms due to the presence of one or more glycines in the RII isoform sequences.[155] These studies are currently in progress and may provide important clues as to the importance of conformationally flexibility in the function of RII versus RI.

B. Hydrogen/Deuterium (H/D) Exchange:Mass Spectrometry

H/D exchange:mass spectrometry involves the measurement of the time course of the replacement of surface-exposed backbone amide hydrogens for deuterium. It involves an initial phase of deuterium incorporation, followed by simultaneous H_2O quenching to stop the reaction and acidification to minimize back exchange, followed by proteolytic fragmentation and mass spectrometry to quantitate deuterium incorporation and peptide identification. The kinetics of replacement are a good measure of solvent accessibility and backbone flexibility of surface segments of proteins in various conformational states. Over the past several years hydrogen/deuterium (H/D) exchange coupled with mass spectrometry has evolved as a powerful method for mapping protein:protein interaction sites as well as ligand-induced or protein-induced conformational changes.[91,162,170,171] In contrast to crystal structures, this method also allows us to map conformation in solution. Unlike time-resolved fluorescence anisotropy where local changes are monitored, H/D mass spectrometry can measure global changes in a comprehensive way. Thus, it is a powerful complement to both the TRFA studies and the crystallography. New methods are being developed that allow for more rapid data collection, for more comprehensive proteolytic coverage of proteins, for higher resolution of the proteolytic mapping, and for improved computational methods to handled the data that is generated. The catalytic subunit of cAPK has been used as a prototype for some of these studies,[170] and the recent work of Anderson et al.[91] has demonstrated specifically that ADP induces changes in the C helix based on H/D exchange. The applications of H/D exchange/mass spectrometry to the regulatory subunits and the AKAPs and to the various molecular complexes is very promising.

C. NMR Spectroscopy

NMR spectroscopy can be used to monitor the dynamics of the entire protein and on a broad range of time scales, from subnanoseconds to days, depending upon the type of NMR experiment employed. Currently, backbone fluctuation information typically comes from heteronuclear ($^{15}N-^{1}H$) relaxation and ^{15}N chemical-shift anisotropy measurements; however, here is an ever-expanding array of methodologies that may yield even more information. Heteronuclear NMR has the obvious advantage of providing high-resolution information of proteins in solution; however, its limitation in the past has been size. The new TROSY methods pioneered by the Wuthrich laboratory are removing those size constraints.[19] Additional technological advances in using heteronuclear labeling of individual components that are part of large molecular assemblies are also providing new opportunities for studying these highly dynamic macromolecular complexes.[172] Cryoprobes are reducing the concentrations of proteins needed for high-resolution data acquisition.

The development of these new methods promises exciting advances in our understanding of protein dynamics over the coming years for the protein kinase family. The availability of high-quality proteins, in large quantity, makes cAPK an excellent candidate to take advantage of these different approaches.

VI. Glossary

ADP adenosine diphosphate

AGC	cAMP-dependent, cGMP-dependent, and PKC subfamily of protein kinases
AKAP	A-kinase anchoring protein
AMPPNP	adenylyl imidodiphosphate
ATP	adenosine triphosphate
C	catalytic subunit
cAMP	adenosine-3′,5′-cyclic monophosphate
cAPK	cAMP-dependent protein kinase
CNB	cyclic nucleotide-binding domain
D/D	dimerization/docking domain
H/D	hydrogen/deuterium
MAP2	microtubule-associated protein 2
NES	nuclear export signal
NMR	nuclear magnetic resonance
PBC	phosphate-binding cassette
PDK1	3-phosphoinositide-dependent protein kinase 1
PKI	heat-stable protein kinase inhibitor
R	regulatory subunit
RI/RII	type I/II regulatory subunit of cAPK
RIα, RIIα, and RIIβ	specific isoforms of the regulatory subunits
(Δ1−91)RIα and (Δ1−91)RIIβ	deletion mutants of the RIα and RIIβ subunits
SDL	site-directed labeling
TRFA	time-resolved fluorescence anisotropy

VII. Acknowledgement

The authors acknowledge the assistance of Ashton Taylor and Drs. Christopher Smith and Yulong Ma for their assistance in preparation of the figures, Nina Haste and Maureen Dawson for preparation of the manuscript, and Drs. Jie Yang and Donald Blumenthal (University of Utah) for their critical reviewing of the manuscript. The work reviewed in this manuscript was supported in part by U.S. Public Health Service Grants GM19301 and GM34921 to S.S.T. as well as by the Howard Hughes Medical Institute. P.A. was supported by USPHS Training Grant DK07541.

VIII. References

(1) Fischer, E. H.; Krebs, E. G. *J. Biol. Chem.* **1955**, *216*, 121.
(2) Hanks, S. K.; Hunter, T. *FASEB J.* **1995**, *8*, 576.
(3) Plowman, G.; Sudarsanam, S.; Bingham, J.; Whyte, D.; Hunter, T. *Proc. Natl. Acad. Sci. U.S.A.* **1999**, *96*, 13603.
(4) Walsh, D. A.; Perkins, J. P.; Krebs, E. G. *J. Biol. Chem.* **1968**, *243*, 3763.
(5) Beebe, S. J.; Corbin, J. D. In *The Enzymes: Control by Phosphorylation Part A*; Krebs, E. G., Boyer, P. D., Eds.; Academic Press: New York, 1986; Vol. XVII, p 43.
(6) Taylor, S. S.; Buechler, J. A.; Yonemoto, W. *Annu. Rev. Biochem.* **1990**, *59*, 971.
(7) Francis, S. H.; Corbin, J. D. *Annu. Rev. Physiol.* **1994**, *56*, 237.
(8) Taylor, S. S.; Knighton, D. R.; Zheng, J.; Ten Eyck, L. F.; Sowadski, J. M. *Annu. Rev. Cell Biol.* **1992**, *8*, 429.
(9) Smith, C. M.; Andzelm, E. R.; Madhusudan; Akamine, P.; Taylor, S. S. *Prog. Biophys. Mol. Biol.* **1999**, *71*, 313.
(10) Gill, G. N.; Garren, L. D. *Biochem. Biophys. Res. Comm.* **1970**, *39*, 335.
(11) Slice, L. W.; Taylor, S. S. *J. Biol. Chem.* **1989**, *264*, 20940.
(12) Saraswat, L. D.; Ringheim, G. A.; Bubis, J.; Taylor, S. S. *J. Biol. Chem.* **1988**, *263*, 18241.
(13) Herberg, F. W.; Taylor, S. S.; Dostmann, W. R. *Biochemistry* **1996**, *35*, 2934.
(14) Colledge, M.; Scott, J. D. *Trends Cell Biol.* **1999**, *9*, 216.
(15) Skalhegg, B. S.; Tasken, K. *Front. Biosci.* **1997**, *2*, 331.
(16) Rubin, C. S. *Biochim. Biophys. Acta* **1994**, *1124*, 467.
(17) Walsh, D. A.; Angelos, K. L.; Van Patten, S. M.; Glass, D. B.; Garetto, L. P. In *Peptides and Protein Phosphorylation*; Kemp, B. E., Ed.; CRC Press: Boca Raton, 1990.
(18) Wen, W.; Meinkoth, J. L.; Tsien, R. Y.; Taylor, S. S. *Cell* **1995**, *82*, 463.
(19) Pervushin, K.; Reik, R.; Wider, G.; Wuthrich, K. *Proc. Natl. Acad. Sci. U.S.A.* **1997**, *94*, 12366.
(20) Knighton, D. R.; Zheng, J.; Ten Eyck, L. F.; Ashford, V. A.; Xuong, N.-h.; Taylor, S. S.; Sowadski, J. M. *Science* **1991**, *253*, 407.
(21) Barker, W. C.; Dayhoff, M. O. *Proc. Natl. Acad. Sci. U.S.A.* **1982**, *79*, 2836.
(22) Hanks, S. K.; Quinn, A. M.; Hunter, T. *Science* **1988**, *241*, 42.
(23) Radzio-Andzelm, E.; Lew, J.; Taylor, S. S. *Structure* **1995**, *3*, 1135.
(24) Taylor, S. S.; Radzio-Andzelm, E. *Structure* **1994**, *2*, 345.
(25) Taylor, S. S.; Radzio-Andzelm, E.; Hunter, T. *FASEB J.* **1995**, *9*, 1255.
(26) Zheng, J.; Knighton, D. R.; Ten Eyck, L. F.; Karlsson, R.; Xuong, N.-h.; Taylor, S. S.; Sowadski, J. M. *Biochemistry* **1993**, *32*, 2154.
(27) Knighton, D. R.; Zheng, J.; Ten Eyck, L. F.; Xuong, N.-h.; Taylor, S. S.; Sowadski, J. M. *Science* **1991**, *253*, 414.
(28) Yonemoto, W.; Garrod, S. M.; Bell, S. M.; Taylor, S. S. *J. Biol. Chem.* **1993**, *268*, 18626.
(29) Bossemeyer, D. *Trends Biochem. Sci.* **1994**, *5*, 201.
(30) Grant, B.; Hemmer, W.; Tsigelny, I.; Adams, J. A.; Taylor, S. S. *Biochemistry* **1998**, *37*, 7708.
(31) Hemmer, W.; McGlone, M. L.; Tsigelny, I.; Taylor, S. S. *J. Biol. Chem.* **1997**, *272*, 16946.
(32) Aimes, R. T.; Hemmer, W.; Taylor, S. S. *Biochemistry* **2000**, *39*, 8325.
(33) Grant, B. D.; Tsigelny, I.; Adams, J. A.; Taylor, S. S. *Protein Sci.* **1996**, *5*, 1316.
(34) Xu, A.; Hawkins, C.; Narayanan, N. *J. Mol. Cell Cardiol.* **1997**, *29*, 405.
(35) Xu, W.; Doshi, A.; Lei, M.; Eck, M.; Harrison, S. *Mol. Cell* **1999**, *5*, 629.
(36) Sicheri, F.; Moarefi, I.; Kuriyan, J. *Nature* **1997**, *385*, 602.
(37) Schindler, T.; Sicheri, F.; Pico, A.; Gazit, A.; Levitzki, A.; Kuriyan, J. *Mol. Cell* **1999**, *5*, 639.
(38) Hubbard, S. R. *EMBO J.* **1997**, *18*, 5572.
(39) Hubbard, S. R.; Wei, L.; Ellis, L.; Hendrickson, W. *Nature* **1994**, *372*, 746.
(40) De Bondt, H. L.; Rosenblatt, J.; Jancarik, J.; Jones, H. D.; Morgan, D. O.; Kim, S. H. *Nature* **1993**, *363*, 595.
(41) Jeffrey, P.; Russo, A.; Polyak, K.; Gibbs, E.; Hurwitz, J.; Massague, J.; Pavletich, N. *Nature* **1995**, *376*, 313.
(42) Russo, A.; Jeffrey, P.; Pavletich, N. *Nat. Struct. Biol.* **1996**, *8*, 696.
(43) Narayana, N.; Cox, S.; Shaltiel, S.; Taylor, S. S.; Xuong, N.-h. *Biochemistry* **1997**, *36*, 4438.
(44) Adams, J. A.; Taylor, S. S. *Biochemistry* **1992**, *31*, 8516.
(45) Zhou, J.; Adams, J. A. *Biochemistry* **1997**, *10*, 22977.
(46) Tsigelny, I.; Greenberg, J.; Cox, S.; Nichols, W.; Taylor, S. S.; Ten Eyck, L. F. *Biopolymers* **1999**, *50*, 513.
(47) Zhang, F.; Strand, A.; Robbins, D.; Cobb, M. H.; Goldsmith, E. J. *Nature* **1994**, *367*, 704.
(48) Johnson, L.; Noble, M.; Owen, D. *Cell* **1996**, *85*, 149.
(49) Cauthron, R. D.; Carter, K. B.; Liauw, S.; Steinberg, R. A. *Mol. Cell Biol.* **1998**, *18*, 1416.
(50) Cheng, X.; Ma, Y.; Moore, M.; Hemmings, B. A.; Taylor, S. S. *Proc. Natl. Acad. Sci. U.S.A.* **1998**, *95*, 9849.
(51) Belham, C.; Wu, S. L.; Avruch, J. *Curr. Biol.* **1999**, *9*, R93.
(52) Kemp, B. E.; Graves, D. J.; Benjamini, E.; Krebs, E. G. *J. Biol. Chem.* **1977**, *252*, 4888.
(53) Karlsson, R.; Zheng, J.; Xuong, N.-h.; Taylor, S. S.; Sowadski, J. M. *Acta Crystallogr.* **1993**, *D49*, 381.
(54) Narayana, N.; Cox, S.; Xuong, N.-h.; Ten Eyck, L. F.; Taylor, S. S. *Structure* **1997**, *5*, 921.
(55) Shaltiel, S.; Cox, S.; Taylor, S. S. *Proc. Natl. Acad. Sci. U.S.A.* **1998**, *95*, 484.
(56) Batkin, M.; Schvartz, I.; Shaltiel, S. *Biochemistry* **2000**, *39*, 5366.
(57) Zheng, J.; Knighton, D. R.; Xuong, N.-h.; Taylor, S. S.; Sowadski, J. M.; Ten Eyck, L. F. *Protein Sci.* **1993**, *2*, 1559.
(58) Veron, M.; Radzio-Andzelm, E.; Tsigelny, I.; Ten Eyck, L. F.; Taylor, S. S. *Proc. Natl. Acad. Sci. U.S.A.* **1993**, *90*, 10618.
(59) Zimmerman, B.; Chiroiani, J.; Ma, Y.; Kotin, R.; Herberg, F. W. *J. Biol. Chem.* **1999**, *274*, 5370.
(60) Gangal, M.; Clifford, T.; Deich, J.; Cheng, X.; Taylor, S. S.; Johnson, D. A. *Proc. Natl. Acad. Sci. U.S.A.* **1999**, *96*, 12394.
(61) McLaughlin, S.; Aderem, A. *Trends Biochem. Sci.* **1995**, *20*, 272.
(62) Resh, M. *Biochim. Biophys. Acta* **1999**, *1451*, 1.
(63) Carr, S. A.; Biemann, K.; Shoji, S.; Parmalee, D. C.; Titani, K. *Proc. Natl. Acad. Sci. U.S.A.* **1982**, *79*, 6128.
(64) Sigal, C.; Zhou, W.; Buser, C.; McLaughlin, J. N.; Resh, M. *Proc. Natl. Acad. Sci. U.S.A.* **1994**, *91*, 12253.
(65) Resh, M. *Biochim. Biophys. Acta* **1994**, *1155*, 307.
(66) Silverman, L.; Resh, M. *J. Cell Biol.* **1992**, *119*, 415.
(67) Ames, J. B.; Ishima, R.; Tanaka, T.; Gordon, J. I.; Stryer, L.; Ikura, M. *Nature* **1997**, *389*, 198.
(68) Tholey, A.; Pipkorn, R.; Bossemeyer, D.; Kinzel, V.; Reed, J. *Biochemistry* **2001**, *40*, 225.

(69) Van Patten, S. M.; Fletcher, W. H.; Walsh, D. A. *J. Biol. Chem.* **1986**, *261*, 5514.
(70) Toner-Webb, J.; van Patten, S. M.; Walsh, D. A.; Taylor, S. S. *J. Biol. Chem.* **1992**, *267*, 25174.
(71) Jedrzejewski, P. T.; Girod, A.; Tholey, A.; König, N.; Thullner, S.; Kinzel, V.; Bossemeyer, D. *Protein Sci.* **1998**, *7*, 457.
(72) Kinzel, V.; Konig, N.; Pipkorn, R.; Bossemeyer, D.; Lehmann, W. *Protein Sci.* **2000**, *11*, 2269.
(73) Yonemoto, W.; Garrod, S. M.; Taylor, S. S. *Protein Eng.* **1997**, *10*, 915.
(74) Shoji, S.; Titani, K.; Demaille, J. G.; Fischer, E. H. *J. Biol. Chem.* **1979**, *254*, 6211.
(75) Aurora, R.; Rose, G. D. *Protein Sci.* **1998**, *7*, 21.
(76) Gaudet, R.; Savage, J. R.; McLaughlin, J. N.; Willardson, B. M.; Sigler, P. B. *Mol. Cell* **1999**, *3*, 649.
(77) Uhler, M. D.; Carmichael, D.; Lee, D.; Chrivia, J.; Krebs, E. G.; McKnight, G. S. *Proc. Natl. Acad. Sci. U.S.A.* **1986**, *83*, 1300.
(78) Showers, M. O.; Maurer, R. A. *J. Biol. Chem.* **1986**, *261*, 16288.
(79) Beebe, S. J.; Salomonsky, P.; Jahnsen, T.; Li, Y. *J. Biol. Chem.* **1992**, *267*, 25505.
(80) Skalhegg, B. S.; Tasken, K. *Front. Biosci.* **2000**, *5*, D678.
(81) San Agustin, J. T.; Wilkerson, C. G.; Witman, G. B. *Mol. Biol. Cell* **2000**, *11*, 3031.
(82) Reinton, N.; Orstavik, S.; Haugen, T.; Jahnsen, T.; Tasken, K.; Skalhegg, B. S. *Biol. Reprod.* **2000**, *63*, 607.
(83) Desseyn, J.-L.; Burton, K. A.; McKnight, G. S. *Proc. Natl. Acad. Sci. U.S.A.* **2000**, *97*, 6433.
(84) Thullner, S.; Gesellchen, F.; Wiemann, S.; Pyerin, W.; Kinzel, V.; Bossemeyer, D. *Biochem. J.* **2000**, *351*, 123.
(85) Guthrie, C.; Skalhegg, B. S.; McKnight, G. S. *J. Biol. Chem.* **1997**, *272*, 29560.
(86) Biondi, R.; Chenung, P.; Casamayor, A.; Deak, M.; Currie, R.; Alessi, D. *EMBO J.* **2000**, *19*, 979.
(87) Shaltiel, S.; Seger, R.; Goldblatt, D. In *The Roots of Modern Biochemistry*; Kleinkauf, von Dohren, Jaenicke, Eds.; de Gruyter & Co.: Berlin, New York, 1988; p 781.
(88) Chestukhin, A.; Litovchick, L.; Muradov, K.; Batkin, M.; Shaltiel, S. *J. Biol. Chem.* **1997**, *272*, 3153.
(89) Stuckey, J.; Schubert, H.; Fauman, E.; Zhang, Z.; Dixon, J.; Saper, M. *Nature* **1994**, *370*, 571.
(90) Fauman, E. B.; Cogswell, J.; Lovejoy, B.; WJ, R.; Holmes, W.; Montana, V.; Piwnica-Worms, H.; Rink, M.; Saper, M. *Cell* **1998**, *93*, 617.
(91) Anderson, M. D.; Shaffer, J.; Jennings, P. A.; Adams, M. R. *J. Biol. Chem.* **2001**, *In Press*.
(92) Gibbs, C. S.; Zoller, M. J. *J. Biol. Chem.* **1991**, *266*, 8923.
(93) Lew, J.; Taylor, S. S.; Adams, J. A. *Biochemistry* **1997**, *36*, 6717.
(94) Shaffer, J.; Adams, J. A. *Biochemistry* **1999**, *38*, 12072.
(95) Shaffer, J.; Adams, J. A. *Biochemistry* **1999**, *38*, 5572.
(96) Hagopian, J.; Kirtley, M.; Stevenson, L.; Gergis, R.; Russo, A.; Pavletich, N.; Parsons, S.; Lew, J. *J. Biol. Chem.* **2001**, *1*, 275.
(97) Gangal, M.; Cox, S.; Lew, J.; Clifford, T.; Garrod, S.; Aschbaher, M.; Taylor, S. S.; Johnson, D. A. *Biochemistry* **1998**, *37*, 13728.
(98) Hauer, J. A.; Barthe, P.; Taylor, S. S.; Parello, J.; Padille, A. *Protein Sci.* **1999**, *8*, 545.
(99) Scott, J. D.; Fischer, E. H.; Demaille, J. G.; Krebs, E. G. *Proc. Natl. Acad. Sci. U.S.A.* **1985**, *82*, 4379.
(100) Cheng, H.-C.; van Patten, S. M.; Smith, A. J.; Walsh, D. A. *Biochem. J.* **1986**, *231*, 655.
(101) Walsh, D. A.; Ashby, C. D.; Gonzalez, C.; Calkins, D.; Fischer, E. H.; Krebs, E. G. *J. Biol. Chem.* **1971**, *246*, 1977.
(102) Scarpetta, M. A.; Uhler, M. D. *J. Biol. Chem.* **1993**, *268*, 10927.
(103) Wen, W.; Taylor, S. S.; Meinkoth, J. L. *J. Biol. Chem.* **1995**, *270*, 2041.
(104) Tash, J.; Welsh, M.; Means, A. *Cell* **1980**, *21*, 57.
(105) Whitehouse, S.; Walsh, D. A. *J. Biol. Chem.* **1983**, *258*, 3682.
(106) Lew, J.; Coruh, N.; Tsigelny, I.; Garrod, S.; Taylor, S. S. *J. Biol. Chem.* **1997**, *272*, 1507.
(107) Herberg, F. W.; Taylor, S. S. *Biochemistry* **1993**, *32*, 14015.
(108) Herberg, F. W.; Doyle, M. L.; Cox, S.; Taylor, S. S. *Biochemistry* **1999**, *38*, 6352.
(109) Padilla, A.; Hauer, J. A.; Tsigelny, I.; Parello, J.; Taylor, S. S. *J. Pept. Res.* **1997**, *49*, 210.
(110) Reed, J.; de Ropp, J. S.; Trewhella, J.; Glass, D. B.; Liddle, W. K.; Bradbury, E. M.; Kinzel, V.; Walsh, D. A. *Biochem. J.* **1989**, *264*, 371.
(111) Thomas, J.; Van Patten, S. M.; Howard, P.; Day, K. H.; Mitchell, R. D.; Sosnick, T.; Trewhella, J.; Walsh, D. A.; Maurer, R. A. *J. Biol. Chem.* **1991**, *266*, 10906.
(112) Reed, J.; Kinzel, V.; Cheng, H.-C.; Walsh, D. A. *Biochemistry* **1987**, *26*, 7641.
(113) Reed, J.; Kinzel, V.; Kemp, B. E.; Cheng, H.-C.; Walsh, D. A. *Biochemistry* **1985**, *24*, 2967.
(114) Hauer, J. A.; Taylor, S. S.; Johnson, B. D. *Biochemistry* **1999**, *38*, 6774.
(115) Cheng, H.-C.; Kemp, B. E.; Pearson, R. B.; Smith, A. J.; Misconi, L.; Van Patten, S. M.; Walsh, D. A. *J. Biol. Chem.* **1986**, *261*, 989.
(116) Jahnsen, T.; Hedin, L.; Kidd, V. J.; Beattie, W. G.; Lohmann, S. M.; Walter, V.; Durica, J.; Schulz, T. Z.; Schlitz, E.; Browner, M.; Lawrence, C. B.; Goldman, D.; Ratoosh, S. L.; Richards, J. S. *J. Biol. Chem.* **1986**, *261(26)*, 12352.
(117) Clegg, C. H.; Codd, G. G.; McKnight, G. S. *Proc. Natl. Acad. Sci. U.S.A.* **1988**, *85*, 3703.
(118) Hofmann, F.; Beavo, J. A.; Bechtel, P. J.; Krebs, E. G. *J. Biol. Chem.* **1975**, *250*, 7795.
(119) Rosen, O. M.; Erlichman, J.; Rubin, C. S. *Adv. Cyclic Nucleotide Res.* **1975**, *5*, 253.
(120) Titani, K.; Sasagawa, T.; Ericsson, L.; Kumar, S.; Smith, S. B.; Krebs, E. G.; Walsh, K. A. *Biochemistry* **1984**, *23*, 4193.
(121) Takio, K.; Smith, S. B.; Krebs, E. G.; Walsh, K. A.; Titani, K. *Biochemistry* **1984**, *23*, 4200.
(122) Geahlen, R. L.; Krebs, E. G. *J. Biol. Chem.* **1980**, *255*, 9375.
(123) Geahlen, R. L.; Krebs, E. G. *J. Biol. Chem.* **1980**, *255*, 1164.
(124) Carmichael, D. F.; Geahlen, R. L.; Allen, S. M.; Krebs, E. G. *J. Biol. Chem.* **1982**, *257*, 10440.
(125) Erlichman, J.; Rosenfeld, R.; Rosen, O. M. *J. Biol. Chem.* **1976**, *251*, 7526.
(126) Chain, D. G.; Hegde, A. N.; Yamamoto, N.; Liu-Marsh, B.; Schwartz, J. H. *J. Neurosci.* **1995**, *15*, 7592.
(127) Herberg, F. W.; Dostmann, W. R. G.; Zorn, M.; Davis, S. J.; Taylor, S. S. *Biochemistry* **1994**, *23*, 7485.
(128) Øgreid, D.; Døskeland, S. O. *FEBS Lett.* **1981**, *129*, 287.
(129) Øgreid, D.; Døskeland, S. O. *FEBS Lett.* **1981**, *129*, 282.
(130) Neitzel, J. J.; Dostmann, W. R. G.; Taylor, S. S. *Biochemistry* **1991**, *30*, 733.
(131) Diller, T. C.; Madhusudan; Xuong, N.-h.; Taylor, S. S. *Structure* **2001**, *9*, 73.
(132) Levin, L. R.; Kuret, J.; Johnson, K. E.; Powers, S.; Cameron, S.; Michaeli, T.; Wigler, M.; Zoller, M. J. *Science* **1988**, *240*, 68.
(133) Gibbs, C. S.; Knighton, D. R.; Sowadski, J. M.; Taylor, S. S.; Zoller, M. J. *J. Biol. Chem.* **1992**, *267*, 4806.
(134) Orellana, S. A.; McKnight, G. S. *J. Biol. Chem.* **1990**, *265*, 3048.
(135) Gibson, R. M.; Ji-Buechler, Y.; Taylor, S. S. *Protein Sci.* **1997**, *6*, 1825.
(136) Gibson, R. M.; Ji-Buechler, Y.; Taylor, S. S. *J. Biol. Chem.* **1997**, *272*, 16343.
(137) Huang, L. J.; Taylor, S. S. *J. Biol. Chem.* **1998**, *273*, 26739.
(138) Bubis, J.; Vedvick, T. S.; Taylor, S. S. *J. Biol. Chem.* **1987**, *262*, 14961.
(139) Banky, P.; Huang, L. J.; Taylor, S. S. *J. Biol. Chem.* **1998**, *273*, 35048.
(140) Su, Y.; Dostmann, W. R. G.; Herberg, F. W.; Durick, K.; Xuong, N.-h.; Ten Eyck, L. F.; Taylor, S. S.; Varughese, K. I. *Science* **1995**, *269*, 807.
(141) Newlon, M. G.; Roy, M.; Morikis, D.; Carr, D. W.; Westphal, R.; Scott, J. D.; Jennings, P. A. *EMBO J.* **2001**, *7*, 1651.
(142) Newlon, M. G.; Roy, M.; Morikis, D.; Hauseken, Z. E.; Coghlan, V.; Scott, J. D.; Jennings, P. A. *Nat. Struct. Biol.* **1999**, *6*, 222.
(143) Shabb, J. B.; Corbin, J. D. *J. Biol. Chem.* **1992**, *267*, 5723.
(144) Weber, I. T.; Shabb, J. B.; Corbin, J. D. *Biochemistry* **1989**, *28*, 6122.
(145) Bonigk, W.; Bradley J.; Muller F.; Sesti F.; Boekhoff I.; Ronnett GV.; Kaupp UB.; Frings S. *J. Neurosci.* **1999**, *19*, 5332.
(146) Nakamura, T.; Gold, G. H. *Nature* **1987**, *325*, 442.
(147) de Rooij, J.; Zwawrtkruis, F. J. T.; Verheijen, M. H. G.; Cool, R. H.; Nijman, S. M. B.; Wittinghofer, A.; Bos, J. L. *Nature* **1998**, *396*, 474.
(148) Kawasaki, H.; Springett, G. M.; Mochizuki, N.; Toki, S.; Nakaya, M.; Matsuda, M.; Housman, D. E.; Graybiel, A. M. *Science* **1998**, *282*, 2275.
(149) Weber, I. T.; Steitz, T. A.; Bubis, J.; Taylor, S. S. *Biochemistry* **1987**, *26*, 343.
(150) Reimann, E. M. *Biochemistry* **1985**, *25*, 119.
(151) León, D. A.; Dostmann, W. R. G.; Taylor, S. S. *Biochemistry* **1991**, *30*, 3035.
(152) León, D. A.; Canaves, J. M.; Taylor, S. S. *Biochemistry* **2000**, *39*, 5662.
(153) Canaves, J. M.; León, D. A.; Taylor, S. S. *Biochemistry* **2000**, *39*, 15022.
(154) Li, F.; Gangal, M.; Jones, J. M.; Deich, J.; Lovett, K.; Taylor, S. S.; Johnson, D. A. *Biochemistry* **2000**, *39*, 15626.
(155) Zhao, J.; Hoye, E.; Boylan, S.; Walsh, D. A.; Trewhella, J. *J. Biol. Chem.* **1998**, *273*, 30448.
(156) Cheng, X.; Phelphs, C.; Taylor, S. S. *J. Biol. Chem.* **2001**, *6*, 4102.
(157) Rubin, C. S. *J. Biol. Chem.* **1979**, *254*, 12439.
(158) Corbin, J. D.; Keely, S. L. *J. Biol. Chem.* **1977**, *252*, 910.
(159) Theuckauf, W. E.; Vallee, R. B. *J. Biol. Chem.* **1982**, *257*, 3284.
(160) Hunter, T. *Cell* **2000**, *100*, 113.
(161) Pawson, T.; Scott, J. D. *Science* **1997**, *278*, 2075.
(162) Herberg, F. W.; Maleszka, A.; Eide, T.; Vossebein, L.; Tasken, K. *J. Mol. Biol.* **2000**, *298*, 329.
(163) Carr, D. W.; Stofko-Hahn, R. E.; Fraser, I. D.; Bishop, S. M.; Acott, T. S.; Brennan, R. G.; Scott, J. D. *J. Biol. Chem.* **1991**, *266*, 14188.
(164) Klauck, T.; Faux, M.; Labudda, K.; Langeberg, L.; Jaken, S.; Scott, J. D. *Science* **1996**, *271*, 1589.

(165) Rosenmund, C.; Carr, D. W.; Bergeson, S.; Nilaver, G.; Scott, J. D.; Westbrook, G. *Nature* **1994**, *368*, 853.
(166) Lester, L.; Langeberg, L.; Scott, J. D. *Proc. Natl. Acad. Sci. U.S.A.* **1997**, *94*, 14942.
(167) Feliciciello, A.; Li, Y.; Avvedimento, E.; Gottesman, M.; Rubin, C. S. *Curr. Biol.* **1997**, *7*, 1011.
(168) Honda, A.; Adams, S.; Sawyer, C.; Lev-Ram, V. V.; Tsien, R.; Dostmann, W. *Proc. Natl. Acad. Sci. U.S.A.* **2001**, *93*, 2437.
(169) Zaccolo, M.; Ge Giorigi, F.; Cho, C.; Feng, L.; Knapp, T.; Negulescu, P.; Taylor, S. S.; Tsien, R. Y.; Pozzan, T. *Nat. Cell Biol.* **2000**, *2*, 25.
(170) Mandell, J. G.; Falick, A. M.; Komives, E. A. *Proc. Natl. Acad. Sci. U.S.A.* **1998**, *95*, 14705.
(171) Mandell, J. G.; Falick, A. M.; Komives, E. A. *Anal. Chem.* **1998**, *70*, 3987.
(172) Takahashi, H.; Nakanishi, T.; Kami, K.; Arata, Y.; Shimada, I. *Nat. Struct. Biol.* **2000**, *7*, 220.
(173) Bossemeyer, D.; Engh, R. A.; Kinzel, V.; Ponstingl, H.; Huber, R. *EMBO J.* **1993**, *12*, 849.
(174) Knighton, D. R.; Bell, S. M.; Zheng, J.; Ten Eyck, L. F.; Xuong, N.-h.; Taylor, S. S.; Sowadski, J. M. *Acta Crystallogr.* **1993**, *D49*, 357.
(175) Prade, L.; Engh, R. A.; Girod, A.; Kinzel, V.; Huber, R.; Bossemeyer, D. *Structure* **1997**, *5*, 1627.
(176) Engh, R. A.; Girod, A.; Kinzel, V.; Huber, R.; Bossemeyer, D. *J. Biol. Chem.* **1996**, *271*, 26157.
(177) Narayana, N.; Diller, T. C.; Koide, K.; Bunnage, M. E.; Nicolaou, K. C.; Brunton, L. L.; Xuong, N.-h.; Ten Eyck, L. F.; Taylor, S. S. *Biochemistry* **1999**, *38*, 2367.
(178) Madhusudan; Trafny, E. A.; Xuong, H.-h.; Adams, J. A.; Ten Eyck, L. F.; Taylor, S. S.; Sowadski, J. M. *Protein Sci.* **1994**, *3*, 176.

CR000226K